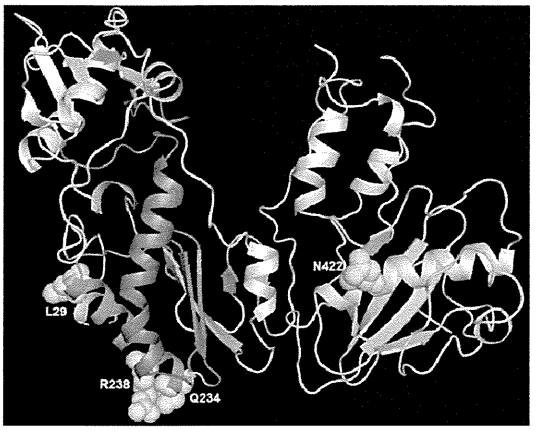

Figure 9. Molecular model of XMRV RT. Ribbons diagram of XMRV RT with the conserved polymerase Motifs color-coded: Motif A (green), B (brown), C (purple), D (red), E (orange) and F (blue). The residues that differ from MoMLV's polymerase domain are shown in ball and stick representation.

information since they were not included in the original crystal structure of MoMLV RT. The differences between XMRV RT and HIV-1 RT are very significant. Unlike the HIV enzyme, XMRV RT appears to be a monomer in solution. Moreover, alignment of the HIV-1 RT–DNA complex with XMRV RT based on their active sites at the palm subdomains shows that the thumb subdomain of XMRV RT would have to be repositioned to be able to accommodate nucleic acid.

DISCUSSION

Early studies reported the presence of XMRV in stromal cells from prostate cancer patient samples and also in CFS clinical samples. Some of the subsequent studies confirmed these findings whereas several others failed to identify XMRV in prostate cancer or in CFS patients, even when same samples were used (71). It was recently reported that human sample contamination with mouse DNA can occur frequently (17,72–74). Moreover, two coauthors from this study have recently demonstrated that XMRV is the product of recombination events between two MLV proviruses, suggesting that XMRV may not be relevant to human disease (18). Nonetheless, XMRV is still an important human retrovirus and comparisons with HIV can provide valuable insights into the fundamental mechanisms of DNA polymerization, RT inhibition and drug resistance. (75).

There is high degree of sequence similarity between the XMRV and MoMLV RTs (95% amino acid identity), and much less so with HIV-1 RT. Based on gel filtration experiments we conclude that unlike HIV-1 RT, but similar to MoMLV RT, XMRV RT exists in solution primarily as a monomer. We also included comparisons with HIV-1 RT in this study as it has been extensively studied and provides an excellent frame of reference.

We report here that there are significant differences in the DNA polymerization efficiency of the three enzymes. Although the polymerase active sites of the XMRV and MoMLV enzymes are almost identical, there is a considerable decrease in the efficiency of nucleotide incorporation by XMRV RT. Most differences in sequence are at the RNase H domain and are likely to affect polymerization by changing the positioning of DNA at the polymerase active site.

We have recently solved the crystal structure of the XMRV RNase H at high resolution (1.5Å) (pdb 3P1G) (Kirby, K.A. *et al.*, submitted for publication). We observed major differences in affinity for nucleic acid that we determined with gel-mobility shift assays and with pre-steady state kinetics. SPR experiments dissected in more detail the specific defect of XMRV RT in binding DNA. Surprisingly, XMRV RT can associate very rapidly with DNA, even more so than HIV-1 RT (Figure 1 and Table 3). However, it dissociates from DNA much faster than the HIV enzyme, resulting in an overall reduced binding affinity. A possible reason for the fast association and dissociation rates of XMRV RT may be the apparent monomeric state, which might offer facile access to the nucleic acid binding cleft, although with less contacts and lower affinity than HIV-1 RT, which is a heterodimer (76,77). This high rate of XMRV RT dissociation from DNA likely contributes to the decreased processivity observed in our study, and may have consequences in the recombination rates of this virus.

Previous sequences of XMRV from prostate cancer tumors showed low variability, suggesting that the virus may have a high fidelity of replication (1,10). Our study demonstrated that HIV-1 RT and MoMLV RT incorporated mismatched nucleotides and extended past the mismatches more efficiently than XMRV RT. Pre-steady state kinetics established that the higher overall fidelity of XMRV RT over MoMLV RT is due to a lower affinity for mismatched nucleotides. When compared to HIV-1 RT, however, XMRV RT has differs in both the nucleotide binding and incorporation steps. Nonetheless, XMRV did not have higher fidelity than a related amphotropic MLV virus or HIV-1 in a cell-based assay. It is possible that the high dNTP concentration in dividing cells can suppress mismatching events. We have previously shown (39) that as nucleotide concentrations vary in different cell lines, this can affect viral susceptibility to NRTIs, and possibly in this case also incorporation of mismatched nucleotides. Additional cell-based studies using multiple cell lines and a large panel of viruses should provide a better understanding of the relation between *in vivo* and *in vitro* fidelity.

Early studies have reported susceptibility of XMRV to some antiretrovirals that have been used in the treatment of HIV infection (53–56). In those studies the compounds were tested at the virus level. To better understand the interactions of inhibitors at their RT target level we tested here the ability of these and several more compounds to block the polymerase activity of XMRV RT. We found that two TDRTIs, EFdA-TP and ENdA-TP were very potent RT inhibitors (IC_{50}s: 0.43 μM and 0.14 μM, respectively). Unlike other NRTIs, these compounds have a 3′ OH group and are known to efficiently inhibit HIV replication by blocking translocation (32,58,78).

Preliminary experiments demonstrated that they also block XMRV RT by the same mechanism (data not shown).

In HIV, moderate resistance to EFdA is conferred by the emergence of the M184V mutation at the conserved X position of the conserved YXDD motif of the polymerase active site. Interestingly, XMRV and MoMLV RTs already have a valine (V223) at this position. This difference is likely to contribute to the better potency of EFdA against HIV-1 RT than XMRV RT or MoMLV RT (57,58). It may also contribute to the decreased ability of XMRV RT to unblock chain-terminated primers, as was also reported for M184V HIV-1 RT (79) and to the enhanced fidelity reported here for XMRV RT, which is also reminiscent of the previously reported high fidelity of M184V HIV-1 RT (80,81). Nonetheless, despite the presence of a Val in the YMDD motif of XMRV RT we found EFdA to inhibit very efficiently replication-competent or pseudotyped XMRV, with submicromolar EC_{50}s (40 and 110 nM, respectively).

Previously, highly potent aptamers were selected to inhibit MoMLV RT (60). We demonstrate here that the three aptamers we tested have varying potency against XMRV RT. Aptamer m.1.1FL was the most potent inhibitor of XMRV RT and MoMLV RT in *in vitro* assays (IC_{50} = 2 and 4 nM, respectively). The fact that XMRV and MoMLV RTs are inhibited by the same aptamers at comparable efficiencies suggests that the RT residues that are different in the two enzymes are not critical to the binding of the aptamer. In contrast, heterodimeric HIV-1 RT has a very different binding cleft and is not inhibited by these aptamers.

Tenofovir is an essential component of HIV therapies and is also a potent inhibitor of XMRV RT. HIV resistance to tenofovir is conferred by a single codon mutation (K65R). HIV-1 RT residue 65 is known to interact with the incoming dNTP or the activated tenofovir analog (tenofovir diphosphate) (82). K65R causes resistance to tenofovir by lowering the k_{pol} for the incorporation of the inhibitor into the nascent DNA. We prepared XMRV RT with the equivalent mutation, K103R, and determined that it has decreased susceptibility to tenofovir. Hence, it is possible for XMRV to develop tenofovir resistance through the same mechanism as HIV-1 RT. HIV resistance to AZT can occur by either decreased binding/incorporation or increased excision of the chain-terminating NRTI (33,83). HIV-1 RTs containing the M41L, D67N, K70R, T215Y/F, K219E/Q mutations show enhanced removal of AZT. Our experiments show that unlike wild-type HIV-1 RT, XMRV RT is not able to excise NRTI-terminated primers. Similarly, it was previously shown that MoMLV RT is not capable of unblocking chain-terminated primers (33).

In HIV, decreased binding of AZT is conferred initially in the presence of the primary Q151M mutation, followed by secondary mutations F77L, A62V, V75I and F116Y (27,47,84). XMRV RT already differs from wild-type HIV-1 RT in the first three of these residues (P104, Q113 and L115 versus A62, V75 and F77) (Table 1). We demonstrated that introducing the primary Q→M mutation at the equivalent XMRV RT site (Q190M) resulted in an enzyme with decreased susceptibility to AZT. Hence, it appears that these residues can confer AZT resistance to XMRV by reduced incorporation of nucleotide analogs, as is the case in HIV-2 (41). At this point we do not know if introduction of as yet unknown mutations could endow XMRV RT with the ability to unblock chain-terminated nucleic acids. The details of the molecular mechanism of XMRV resistance to tenofovir and AZT are under investigation.

In conclusion, our study provides detailed biochemical analysis of the mechanisms of polymerization, inhibition, fidelity, processivity and drug resistance of XMRV RT and how it compares with the closely related enzyme MoMLV RT and the more distantly related HIV-1 RT. The findings enhance our understanding of the basic mechanisms of reverse transcription.

SUPPLEMENTARY DATA

Supplementary Data are available at NAR Online.

ACKNOWLEDGEMENTS

The content of this publication does not necessarily reflect the views or policies of the Department of Health Human Services, nor does mention of trade names, commercial products or organizations imply endorsement by the U.S. Government.

FUNDING

NIH grants (AI076119, AI079801, and AI094715, to S.G.S.), (AI074389, to D.H.B.), (AI079801 to M.A.P.); NIH Bench-to-Bedside Award and the Intramural Research Program of the NIH, National Cancer Institute, Center for Cancer Research (to V.K.P); Ministry of Knowledge and Economy, Bilateral International Collaborative R&D Program, Republic of Korea; Canadian Institutes of Health Research (CIHR) and University of Missouri (to S-L.L.); amfAR Mathilde Krim Fellowship and a CIHR Fellowship (to B.M.). Funding for open access charge: NIH grants (AI076119, AI094715, AI074389, AI079801).

Conflict of interest statement. None declared.

REFERENCES

1. Urisman,A., Molinaro,R.J., Fischer,N., Plummer,S.J., Casey,G., Klein,E.A., Malathi,K., Magi-Galluzzi,C., Tubbs,R.R., Ganem,D. *et al.* (2006) Identification of a novel gammaretrovirus in prostate tumors of patients homozygous for R462Q RNASEL variant. *PLoS Pathog.*, **2**, e25.
2. Malathi,K., Dong,B., Gale,M. Jr. and Silverman,R.H. (2007) Small self-RNA generated by RNase L amplifies antiviral innate immunity. *Nature*, **448**, 816–819.
3. Arnold,R.S., Makarova,N.V., Osunkoya,A.O., Suppiah,S., Scott,T.A., Johnson,N.A., Bhosle,S.M., Liotta,D., Hunter,E., Marshall,F.F. *et al.* XMRV infection in patients with prostate cancer: novel serologic assay and correlation with PCR and FISH. *Urology*, **75**, 755–761.
4. Dong,B., Kim,S., Hong,S., Das Gupta,J., Malathi,K., Klein,E.A., Ganem,D., Derisi,J.L., Chow,S.A. and Silverman,R.H. (2007) An

infectious retrovirus susceptible to an IFN antiviral pathway from human prostate tumors. *Proc Natl Acad Sci. USA*, **104**, 1655–1660.
5. Knouf,E.C., Metzger,M.J., Mitchell,P.S., Arroyo,J.D., Chevillet,J.R., Tewari,M. and Miller,A.D. (2009) Multiple integrated copies and high-level production of the human retrovirus XMRV (xenotropic murine leukemia virus-related virus) from 22Rv1 prostate carcinoma cells. *J. Virol.*, **83**, 7353–7356.
6. Schlaberg,R., Choe,D.J., Brown,K.R., Thaker,H.M. and Singh,I.R. (2009) XMRV is present in malignant prostatic epithelium and is associated with prostate cancer, especially high-grade tumors. *Proc. Natl Acad. Sci. USA*, **106**, 16351–16356.
7. Sabunciyan,S., Mandelberg,N., Rabkin,C.S., Yolken,R. and Viscidi,R. No difference in antibody titers against xenotropic MLV related virus in prostate cancer cases and cancer-free controls. *Mol. Cell. Probes.*, **25**, 134–136.
8. Verhaegh,G.W., de Jong,A.S., Smit,F.P., Jannink,S.A., Melchers,W.J. and Schalken,J.A. (2011) Prevalence of human xenotropic murine leukemia virus-related gammaretrovirus (XMRV) in Dutch prostate cancer patients. *Prostate*, **71**, 415–420.
9. Hohn,O., Krause,H., Barbarotto,P., Niederstadt,L., Beimforde,N., Denner,J., Miller,K., Kurth,R. and Bannert,N. (2009) Lack of evidence for xenotropic murine leukemia virus-related virus(XMRV) in German prostate cancer patients. *Retrovirology*, **6**, 92.
10. Lombardi,V.C., Ruscetti,F.W., Das Gupta,J., Pfost,M.A., Hagen,K.S., Peterson,D.L., Ruscetti,S.K., Bagni,R.K., Petrow-Sadowski,C., Gold,B. *et al.* (2009) Detection of an infectious retrovirus, XMRV, in blood cells of patients with chronic fatigue syndrome. *Science*, **326**, 585–589.
11. Henrich,T.J., Li,J.Z., Felsenstein,D., Kotton,C.N., Plenge,R.M., Pereyra,F., Marty,F.M., Lin,N.H., Grazioso,P., Crochiere,D.M. *et al.* (2010) Xenotropic murine leukemia virus-related virus prevalence in patients with chronic fatigue syndrome or chronic immunomodulatory conditions. *J. Infect. Dis.*, **202**, 1478–1481.
12. Erlwein,O., Kaye,S., McClure,M.O., Weber,J., Wills,G., Collier,D., Wessely,S. and Cleare,A. (2010) Failure to detect the novel retrovirus XMRV in chronic fatigue syndrome. *PLoS ONE*, **5**, e8519.
13. Groom,H.C., Boucherit,V.C., Makinson,K., Randal,E., Baptista,S., Hagan,S., Gow,J.W., Mattes,F.M., Breuer,J., Kerr,J.R. *et al.* (2010) Absence of xenotropic murine leukaemia virus-related virus in UK patients with chronic fatigue syndrome. *Retrovirology*, **7**, 10.
14. Switzer,W.M., Jia,H., Hohn,O., Zheng,H., Tang,S., Shankar,A., Bannert,N., Simmons,G., Hendry,R.M., Falkenberg,V.R. *et al.* (2010) Absence of evidence of xenotropic murine leukemia virus-related virus infection in persons with chronic fatigue syndrome and healthy controls in the United States. *Retrovirology*, **7**, 57.
15. Satterfield,B.C., Garcia,R.A., Jia,H., Tang,S., Zheng,H. and Switzer,W.M. (2011) Serologic and PCR testing of persons with chronic fatigue syndrome in the United States shows no association with xenotropic or polytropic murine leukemia virus-related viruses. *Retrovirology*, **8**, 12.
16. Menendez-Arias,L. Evidence and controversies on the role of XMRV in prostate cancer and chronic fatigue syndrome. *Rev. Med. Virol.*, **21**, 3–17.
17. Hue,S., Gray,E.R., Gall,A., Katzourakis,A., Tan,C.P., Houldcroft,C.J., McLaren,S., Pillay,D., Futreal,A., Garson,J.A. *et al.* (2010) Disease-associated XMRV sequences are consistent with laboratory contamination. *Retrovirology*, **7**, 111.
18. Paprotka,T., Delviks-Frankenberry,K.A., Cingoz,O., Martinez,A., Kung,H.J., Tepper,C.G., Hu,W.S., Fivash,M.J. Jr., Coffin,J.M. and Pathak,V.K. (2011) Recombinant origin of the retrovirus XMRV. *Science*, **333**, 97–101.
19. Singh,K., Kaushik,N., Jin,J., Madhusudanan,M. and Modak,M.J. (2000) Role of Q190 of MuLV RT in ddNTP resistance and fidelity of DNA synthesis: a molecular model of interactions with substrates. *Protein Eng.*, **13**, 635–643.
20. Telesnitsky,A. and Goff,S.P. (1993) Two defective forms of reverse transcriptase can complement to restore retroviral infectivity. *EMBO J.*, **12**, 4433–4438.
21. Georgiadis,M.M., Jessen,S.M., Ogata,C.M., Telesnitsky,A., Goff,S.P. and Hendrickson,W.A. (1995) Mechanistic implications from the structure of a catalytic fragment of Moloney murine leukemia virus reverse transcriptase. *Structure*, **3**, 879–892.
22. Das,D. and Georgiadis,M.M. (2004) The crystal structure of the monomeric reverse transcriptase from Moloney murine leukemia virus. *Structure*, **12**, 819–829.
23. Chowdhury,K., Kaushik,N., Pandey,V.N. and Modak,M.J. (1996) Elucidation of the role of Arg 110 of murine leukemia virus reverse transcriptase in the catalytic mechanism: biochemical characterization of its mutant enzymes. *Biochemistry*, **35**, 16610–16620.
24. Kaushik,N., Chowdhury,K., Pandey,V.N. and Modak,M.J. (2000) Valine of the YVDD motif of moloney murine leukemia virus reverse transcriptase: role in the fidelity of DNA synthesis. *Biochemistry*, **39**, 5155–5165.
25. Jacobo-Molina,A., Ding,J., Nanni,R.G., Clark,A.D. Jr., Lu,X., Tantillo,C., Williams,R.L., Kamer,G., Ferris,A.L., Clark,P. *et al.* (1993) Crystal structure of human immunodeficiency virus type 1 reverse transcriptase complexed with double-stranded DNA at 3.0 A resolution shows bent DNA. *Proc. Natl Acad. Sci. USA*, **90**, 6320–6324.
26. Kohlstaedt,L.A., Wang,J., Friedman,J.M., Rice,P.A. and Steitz,T.A. (1992) Crystal structure at 3.5 A resolution of HIV-1 reverse transcriptase complexed with an inhibitor. *Science*, **256**, 1783–1790.
27. Sarafianos,S.G., Marchand,B., Das,K., Himmel,D.M., Parniak,M.A., Hughes,S.H. and Arnold,E. (2009) Structure and function of HIV-1 reverse transcriptase: molecular mechanisms of polymerization and inhibition. *J. Mol. Biol.*, **385**, 693–713.
28. Singh,K., Marchand,B., Kirby,K.A., Michailidis,E. and Sarafianos,S.G. (2010) Structural aspects of drug resistance and inhibition of HIV-1 reverse transcriptase. *Viruses*, **2**, 606–638.
29. Schuckmann,M.M., Marchand,B., Hachiya,A., Kodama,E.N., Kirby,K.A., Singh,K. and Sarafianos,S.G. (2010) The N348I mutation at the connection subdomain of HIV-1 reverse transcriptase decreases binding to nevirapine. *J. Biol. Chem.*, **285**, 38700–38709.
30. Telesnitsky,A. and Goff,S.P. (1993) RNase H domain mutations affect the interaction between Moloney murine leukemia virus reverse transcriptase and its primer-template. *Proc. Natl Acad. Sci. USA*, **90**, 1276–1280.
31. Bauman,J.D., Das,K., Ho,W.C., Baweja,M., Himmel,D.M., Clark,A.D. Jr., Oren,D.A., Boyer,P.L., Hughes,S.H., Shatkin,A.J. *et al.* (2008) Crystal engineering of HIV-1 reverse transcriptase for structure-based drug design. *Nucleic Acids Res.*, **36**, 5083–5092.
32. Michailidis,E., Marchand,B., Kodama,E.N., Singh,K., Matsuoka,M., Kirby,K.A., Ryan,E.M., Sawani,A.M., Nagy,E., Ashida,N. *et al.* (2009) Mechanism of inhibition of HIV-1 reverse transcriptase by 4′-Ethynyl-2-fluoro-2′-deoxyadenosine triphosphate, a translocation-defective reverse transcriptase inhibitor. *J. Biol. Chem.*, **284**, 35681–35691.
33. Meyer,P.R., Matsuura,S.E., So,A.G. and Scott,W.A. (1998) Unblocking of chain-terminated primer by HIV-1 reverse transcriptase through a nucleotide-dependent mechanism. *Proc. Natl Acad. Sci. USA*, **95**, 13471–13476.
34. Halvas,E.K., Svarovskaia,E.S. and Pathak,V.K. (2000) Development of an in vivo assay to identify structural determinants in murine leukemia virus reverse transcriptase important for fidelity. *J Virol*, **74**, 312–319.
35. Patel,S.S., Wong,I. and Johnson,K.A. (1991) Pre-steady-state kinetic analysis of processive DNA replication including complete characterization of an exonuclease-deficient mutant. *Biochemistry*, **30**, 511–525.
36. Sarafianos,S.G., Clark,A.D. Jr., Das,K., Tuske,S., Birktoft,J.J., Ilankumaran,P., Ramesha,A.R., Sayer,J.M., Jerina,D.M., Boyer,P.L. *et al.* (2002) Structures of HIV-1 reverse transcriptase with pre- and post-translocation AZTMP-terminated DNA. *EMBO J.*, **21**, 6614–6624.
37. Tuske,S., Sarafianos,S.G., Clark,A.D. Jr., Ding,J., Naeger,L.K., White,K.L., Miller,M.D., Gibbs,C.S., Boyer,P.L., Clark,P. *et al.* (2004) Structures of HIV-1 RT-DNA complexes before and after

incorporation of the anti-AIDS drug tenofovir. *Nat. Struct. Mol. Biol.*, **11**, 469–474.
38. Sarafianos,S.G., Pandey,V.N., Kaushik,N. and Modak,M.J. (1995) Site-directed mutagenesis of arginine 72 of HIV-1 reverse transcriptase. Catalytic role and inhibitor sensitivity. *J. Biol. Chem.*, **270**, 19729–19735.
39. Hachiya,A., Kodama,E.N., Schuckmann,M.M., Kirby,K.A., Michailidis,E., Sakagami,Y., Oka,S., Singh,K. and Sarafianos,S.G. (2011) K70Q adds high-level tenofovir resistance to "Q151M complex" HIV reverse transcriptase through the enhanced discrimination mechanism. *PLoS One*, **6**, e16242.
40. Sarafianos,S.G., Das,K., Ding,J., Boyer,P.L., Hughes,S.H. and Arnold,E. (1999) Touching the heart of HIV-1 drug resistance: the fingers close down on the dNTP at the polymerase active site. *Chem. Biol.*, **6**, R137–R146.
41. Boyer,P.L., Sarafianos,S.G., Clark,P.K., Arnold,E. and Hughes,S.H. (2006) Why do HIV-1 and HIV-2 use different pathways to develop AZT resistance? *PLoS Pathog.*, **2**, e10.
42. Powell,M.D., Ghosh,M., Jacques,P.S., Howard,K.J., Le Grice,S.F. and Levin,J.G. (1997) Alanine-scanning mutations in the "primer grip" of p66 HIV-1 reverse transcriptase result in selective loss of RNA priming activity. *J. Biol. Chem.*, **272**, 13262–13269.
43. Sarafianos,S.G., Das,K., Clark,A.D. Jr., Ding,J., Boyer,P.L., Hughes,S.H. and Arnold,E. (1999) Lamivudine (3TC) resistance in HIV-1 reverse transcriptase involves steric hindrance with beta-branched amino acids. *Proc. Natl Acad. Sci. USA*, **96**, 10027–10032.
44. Boucher,C.A., Cammack,N., Schipper,P., Schuurman,R., Rouse,P., Wainberg,M.A. and Cameron,J.M. (1993) High-level resistance to (-) enantiomeric 2′-deoxy-3′-thiacytidine in vitro is due to one amino acid substitution in the catalytic site of human immunodeficiency virus type 1 reverse transcriptase. *Antimicrob. Agents Chemother.*, **37**, 2231–2234.
45. Tisdale,M., Kemp,S.D., Parry,N.R. and Larder,B.A. (1993) Rapid in vitro selection of human immunodeficiency virus type 1 resistant to 3′-thiacytidine inhibitors due to a mutation in the YMDD region of reverse transcriptase. *Proc. Natl Acad. Sci. USA*, **90**, 5653–5656.
46. Menendez-Arias,L. (2010) Molecular basis of human immunodeficiency virus drug resistance: an update. *Antiviral Res.*, **85**, 210–231.
47. Sarafianos,S.G., Das,K., Hughes,S.H. and Arnold,E. (2004) Taking aim at a moving target: designing drugs to inhibit drug-resistant HIV-1 reverse transcriptases. *Curr. Opin. Struct. Biol.*, **14**, 716–730.
48. Menendez-Arias,L. (2010) Molecular basis of human immunodeficiency virus drug resistance: an update. *Antiviral Res.*, **85**, 210–231.
49. Menendez-Arias,L. and Berkhout,B. (2008) Retroviral reverse transcription. *Virus Res.*, **134**, 1–3.
50. Shi,Q., Singh,K., Srivastava,A., Kaushik,N. and Modak,M.J. (2002) Lysine 152 of MuLV reverse transcriptase is required for the integrity of the active site. *Biochemistry*, **41**, 14831–14842.
51. Johnson,K.A. (1993) Conformational coupling in DNA polymerase fidelity. *Annu. Rev. Biochem.*, **62**, 685–713.
52. Rezende,L.F. and Prasad,V.R. (2004) Nucleoside-analog resistance mutations in HIV-1 reverse transcriptase and their influence on polymerase fidelity and viral mutation rates. *Int. J. Biochem. Cell Biol.*, **36**, 1716–1734.
53. Paprotka,T., Venkatachari,N.J., Chaipan,C., Burdick,R., Delviks-Frankenberry,K.A., Hu,W.S. and Pathak,V.K. Inhibition of xenotropic murine leukemia virus-related virus by APOBEC3 proteins and antiviral drugs. *J. Virol.*, **84**, 5719–5729.
54. Sakuma,R., Sakuma,T., Ohmine,S., Silverman,R.H. and Ikeda,Y. (2010) Xenotropic murine leukemia virus-related virus is susceptible to AZT. *Virology*, **397**, 1–6.
55. Singh,I.R., Gorzynski,J.E., Drobysheva,D., Bassit,L. and Schinazi,R.F. (2010) Raltegravir is a potent inhibitor of XMRV, a virus implicated in prostate cancer and chronic fatigue syndrome. *PLoS One*, **5**, e9948.
56. Smith,R.A., Gottlieb,G.S. and Miller,A.D. (2010) Susceptibility of the human retrovirus XMRV to antiretroviral inhibitors. *Retrovirology*, **7**, 70.
57. Kawamoto,A., Kodama,E., Sarafianos,S.G., Sakagami,Y., Kohgo,S., Kitano,K., Ashida,N., Iwai,Y., Hayakawa,H., Nakata,H. *et al.* (2008) 2′-deoxy-4′-C-ethynyl-2-halo-adenosines active against drug-resistant human immunodeficiency virus type 1 variants. *Int. J. Biochem. Cell Biol.*, **40**, 2410–2420.
58. Kodama,E.I., Kohgo,S., Kitano,K., Machida,H., Gatanaga,H., Shigeta,S., Matsuoka,M., Ohrui,H. and Mitsuya,H. (2001) 4′-Ethynyl nucleoside analogs: potent inhibitors of multidrug-resistant human immunodeficiency virus variants in vitro. *Antimicrob. Agents Chemother.*, **45**, 1539–1546.
59. Kissel,J.D., Held,D.M., Hardy,R.W. and Burke,D.H. (2007) Single-stranded DNA aptamer RT1t49 inhibits RT polymerase and RNase H functions of HIV type 1, HIV type 2, and SIVCPZ RTs. *AIDS Res. Hum. Retroviruses.*, **23**, 699–708.
60. Chen,H. and Gold,L. (1994) Selection of high-affinity RNA ligands to reverse transcriptase: inhibition of cDNA synthesis and RNase H activity. *Biochemistry*, **33**, 8746–8756.
61. Joshi,P.J., Fisher,T.S. and Prasad,V.R. (2003) Anti-HIV inhibitors based on nucleic acids: emergence of aptamers as potent antivirals. *Curr. Drug Targets Infect. Disord.*, **3**, 383–400.
62. DeStefano,J.J. and Nair,G.R. (2008) Novel aptamer inhibitors of human immunodeficiency virus reverse transcriptase. *Oligonucleotides*, **18**, 133–144.
63. DeStefano,J.J. and Cristofaro,J.V. (2006) Selection of primer-template sequences that bind human immunodeficiency virus reverse transcriptase with high affinity. *Nucleic Acids Res.*, **34**, 130–139.
64. Arion,D., Kaushik,N., McCormick,S., Borkow,G. and Parniak,M.A. (1998) Phenotypic mechanism of HIV-1 resistance to 3′-azido-3′-deoxythymidine (AZT): increased polymerization processivity and enhanced sensitivity to pyrophosphate of the mutant viral reverse transcriptase. *Biochemistry*, **37**, 15908–15917.
65. Sarafianos,S.G., Hughes,S.H. and Arnold,E. (2004) Designing anti-AIDS drugs targeting the major mechanism of HIV-1 RT resistance to nucleoside analog drugs. *Int. J. Biochem. Cell Biol.*, **36**, 1706–1715.
66. Shafer,R.W., Kozal,M.J., Winters,M.A., Iversen,A.K., Katzenstein,D.A., Ragni,M.V., Meyer,W.A. 3rd, Gupta,P., Rasheed,S., Coombs,R. *et al.* (1994) Combination therapy with zidovudine and didanosine selects for drug-resistant human immunodeficiency virus type 1 strains with unique patterns of pol gene mutations. *J. Infect. Dis.*, **169**, 722–729.
67. Shirasaka,T., Kavlick,M.F., Ueno,T., Gao,W.Y., Kojima,E., Alcaide,M.L., Chokekijchai,S., Roy,B.M., Arnold,E., Yarchoan,R. *et al.* (1995) Emergence of human immunodeficiency virus type 1 variants with resistance to multiple dideoxynucleosides in patients receiving therapy with dideoxynucleosides. *Proc. Natl Acad. Sci. USA*, **92**, 2398–2402.
68. Iversen,A.K., Shafer,R.W., Wehrly,K., Winters,M.A., Mullins,J.I., Chesebro,B. and Merigan,T.C. (1996) Multidrug-resistant human immunodeficiency virus type 1 strains resulting from combination antiretroviral therapy. *J. Virol.*, **70**, 1086–1090.
69. Winters,M.A., Shafer,R.W., Jellinger,R.A., Mamtora,G., Gingeras,T. and Merigan,T.C. (1997) Human immunodeficiency virus type 1 reverse transcriptase genotype and drug susceptibility changes in infected individuals receiving dideoxyinosine monotherapy for 1 to 2 years. *Antimicrob. Agents Chemother.*, **41**, 757–762.
70. Gu,Z., Gao,Q., Fang,H., Salomon,H., Parniak,M.A., Goldberg,E., Cameron,J. and Wainberg,M.A. (1994) Identification of a mutation at codon 65 in the IKKK motif of reverse transcriptase that encodes human immunodeficiency virus resistance to 2′,3′-dideoxycytidine and 2′,3′-dideoxy-3′-thiacytidine. *Antimicrob. Agents Chemother.*, **38**, 275–281.
71. Knox,K., Carrigan,D., Simmons,G., Teque,F., Zhou,Y., Hackett,J. Jr., Qiu,X., Luk,K.C., Schochetman,G., Knox,A. *et al.* (2011) No evidence of murine-like gammaretroviruses in CFS patients previously identified as XMRV-infected. *Science*.
72. Oakes,B., Tai,A.K., Cingoz,O., Henefield,M.H., Levine,S., Coffin,J.M. and Huber,B.T. (2010) Contamination of human DNA samples with mouse DNA can lead to false detection of XMRV-like sequences. *Retrovirology*, **7**, 109.
73. Robinson,M.J., Erlwein,O.W., Kaye,S., Weber,J., Cingoz,O., Patel,A., Walker,M.M., Kim,W.J., Uiprasertkul,M., Coffin,J.M.

et al. (2010) Mouse DNA contamination in human tissue tested for XMRV. *Retrovirology*, **7**, 108.
74. Sato,E., Furuta,R.A. and Miyazawa,T. (2010) An endogenous murine leukemia viral genome contaminant in a commercial RT-PCR kit is amplified using standard primers for XMRV. *Retrovirology*, **7**, 110.
75. Coffin,J.M. and Stoye,J.P. (2009) Virology. A new virus for old diseases? *Science*, **326**, 530–531.
76. Huang,H., Chopra,R., Verdine,G.L. and Harrison,S.C. (1998) Structure of a covalently trapped catalytic complex of HIV-1 reverse transcriptase: implications for drug resistance. *Science*, **282**, 1669–1675.
77. Sarafianos,S.G., Das,K., Tantillo,C., Clark,A.D. Jr., Ding,J., Whitcomb,J.M., Boyer,P.L., Hughes,S.H. and Arnold,E. (2001) Crystal structure of HIV-1 reverse transcriptase in complex with a polypurine tract RNA:DNA. *EMBO J.*, **20**, 1449–1461.
78. Kirby,K.A., Singh,K., Michailidis,E., Marchand,B., Kodama,E.N., Ashida,N., Mitsuya,H., Parniak,M.A. and Sarafianos,S.G. The sugar ring conformation of 4′-ethynyl-2-fluoro-2′-deoxyadenosine and its recognition by the polymerase active site of hiv reverse transcriptase. *Cell Mol. Biol.*, **57**, 40–46.
79. Gotte,M., Arion,D., Parniak,M.A. and Wainberg,M.A. (2000) The M184V mutation in the reverse transcriptase of human immunodeficiency virus type 1 impairs rescue of chain-terminated DNA synthesis. *J. Virol.*, **74**, 3579–3585.
80. Wainberg,M.A., Drosopoulos,W.C., Salomon,H., Hsu,M., Borkow,G., Parniak,M., Gu,Z., Song,Q., Manne,J., Islam,S. *et al.* (1996) Enhanced fidelity of 3TC-selected mutant HIV-1 reverse transcriptase. *Science*, **271**, 1282–1285.
81. Pandey,V.N., Kaushik,N., Rege,N., Sarafianos,S.G., Yadav,P.N. and Modak,M.J. (1996) Role of methionine 184 of human immunodeficiency virus type-1 reverse transcriptase in the polymerase function and fidelity of DNA synthesis. *Biochemistry*, **35**, 2168–2179.
82. Das,K., Bandwar,R.P., White,K.L., Feng,J.Y., Sarafianos,S.G., Tuske,S., Tu,X., Clark,A.D. Jr., Boyer,P.L., Hou,X. *et al.* (2009) Structural basis for the role of the K65R mutation in HIV-1 reverse transcriptase polymerization, excision antagonism, and tenofovir resistance. *J. Biol. Chem.*, **284**, 35092–35100.
83. Meyer,P.R., Matsuura,S.E., Mian,A.M., So,A.G. and Scott,W.A. (1999) A mechanism of AZT resistance: an increase in nucleotide-dependent primer unblocking by mutant HIV-1 reverse transcriptase. *Mol. Cell.*, **4**, 35–43.
84. Ueno,T., Shirasaka,T. and Mitsuya,H. (1995) Enzymatic characterization of human immunodeficiency virus type 1 reverse transcriptase resistant to multiple 2′,3′-dideoxynucleoside 5′-triphosphates. *J. Biol. Chem.*, **270**, 23605–23611.
85. Rhee,S.Y., Gonzales,M.J., Kantor,R., Betts,B.J., Ravela,J. and Shafer,R.W. (2003) Human immunodeficiency virus reverse transcriptase and protease sequence database. *Nucleic Acids Res.*, **31**, 298–303.

Biochemical and Biophysical Research Communications 424 (2012) 257–261

Contents lists available at SciVerse ScienceDirect

Biochemical and Biophysical Research Communications

journal homepage: www.elsevier.com/locate/ybbrc

A simple, rapid, and sensitive system for the evaluation of anti-viral drugs in rats

Xiaoguang Li [a,b,f], Hua Qian [a,f], Fusako Miyamoto [a], Takeshi Naito [c], Kumi Kawaji [a], Kazumi Kajiwara [d,e], Toshio Hattori [a], Masao Matsuoka [c], Kentaro Watanabe [d], Shinya Oishi [d], Nobutaka Fujii [d], Eiichi N. Kodama [a,c,*]

[a] Tohoku University Graduate School of Medicine, Department of Internal Medicine/Division of Emerging Infectious Diseases, Sendai 980-8575, Japan
[b] Department of Medical Microbiology, Harbin Medical University, Harbin 150086, China
[c] Laboratory of Virus Control, Institute for Virus Research, Kyoto University, 53 Kawaramachi, Shogoin, Sakyo-ku, Kyoto 606-8507, Japan
[d] Graduate School of Pharmaceutical Sciences, Kyoto University, Sakyo-ku, Kyoto 606-8501, Japan
[e] JST Innovation Plaza Kyoto, Japan Science and Technology Agency, Nishigyo-ku, Kyoto 615-8245, Japan
[f] Center for AIDS Research, Kumamoto University, 2-2-1 Honjo, Kumamoto 860-0811, Japan

ARTICLE INFO

Article history:
Received 6 June 2012
Available online 23 June 2012

Keywords:
HIV-1
MAGI assay
Rat
CXCR4 antagonist
Fusion inhibitor

ABSTRACT

The lack of small animal models for the evaluation of anti-human immunodeficiency virus type 1 (HIV-1) agents hampers drug development. Here, we describe the establishment of a simple and rapid evaluation system in a rat model without animal infection facilities. After intraperitoneal administration of test drugs to rats, antiviral activity in the sera was examined by the MAGI assay. Recently developed inhibitors for HIV-1 entry, two CXCR4 antagonists, TF14016 and FC131, and four fusion inhibitors, T-20, T-20EK, SC29EK, and TRI-1144, were evaluated using HIV-1_{IIIB} and HIV-1_{BaL} as representative CXCR4- and CCR5-tropic HIV-1 strains, respectively. CXCR4 antagonists were shown to only possess anti-HIV-1_{IIIB} activity, whereas fusion inhibitors showed both anti-HIV-1_{IIIB} and anti-HIV-1_{BaL} activities in rat sera. These results indicate that test drugs were successfully processed into the rat sera and could be detected by the MAGI assay. In this system, TRI-1144 showed the most potent and sustained antiviral activity. Sera from animals not administered drugs showed substantial anti-HIV-1 activity, indicating that relatively high dose or activity of the test drugs might be needed. In conclusion, the novel rat system established here, "phenotypic drug evaluation", may be applicable for the evaluation of various antiviral drugs *in vivo*.

1. Introduction

Numerous antiviral agents have been developed to suppress infection with viruses such as human immunodeficiency virus type 1 (HIV-1) [1], and have successfully provided excellent outcomes *in vivo*. However, the emergence of drug-resistant HIV-1 variants is a major concern in HIV therapy. Therefore, the development of novel drugs with sustained activity to resistant variants is desirable. Drugs, especially those targeting HIV-1 entry, have been recently developed and approved, such as a CCR5 antagonist, maraviroc [2], and a fusion inhibitor, enfuvirtide (T-20) [3], where both drugs effectively suppress HIV-1 in the patient even resistant to previous drugs [4,5].

In addition to CCR5, which is a main co-receptor for clinical HIV-1 strains, CXCR4 can also act as a co-receptor for HIV-1 (X4-tropic HIV-1), such as that seen for the vast majority of laboratory-adapted HIV-1 strains [6]. Thus, CXCR4 is also considered an important therapeutic target. We previously identified a β-sheet-like 14-residue peptide, T140 [7,8], and its down-sized analog, a cyclic pentapeptide FC131 (Fig. 1) [9], as potent and specific CXCR4 antagonists. Both T140 and FC131 were proved to inhibit X4-tropic HIV-1 infection *in vitro*. T140 has been further modified to TF14016 (4F-benzoyl-TN14003; BKT140) that shows more potent inhibitory effect [10].

The first fusion inhibitor, T-20, efficiently inhibits replication of HIV-1 resistant even to inhibitors for reverse transcriptase and protease [11,12]. However, the genetic barrier to overcome suppression by T-20 seems to not be high since a 1–2 amino acid(s) substitution in gp41 appears to be sufficient for resistance [13–15]. Therefore, we developed T-20EK [16] and SC29EK [17] as novel and potent fusion inhibitors that sustain their inhibitory effects on T-20 resistant HIV-1 stains. A series of systematic replacements with hydrophilic glutamic acid (E) or lysine (K) was introduced (EK motif) at the solvent-accessible site to enhance the α-helicity of the peptides by possible intrahelical electrostatic interactions [18]. T-20EK/S138A [16] was synthesized

* Corresponding author at: Tohoku University Graduate School of Medicine, Department of Internal Medicine/Division of Emerging Infectious Diseases, Building 1 Room 515, 2-1 Seiryo cho, Aoba-ku, Sendai 980-8575, Japan. Fax: +81 22 717 8221.
E-mail addresses: kodama515@med.tohoku.ac.jp, kodausa21@gmail.com (E.N. Kodama).

0006-291X/$ - see front matter © 2012 Elsevier Inc. All rights reserved.
http://dx.doi.org/10.1016/j.bbrc.2012.06.097

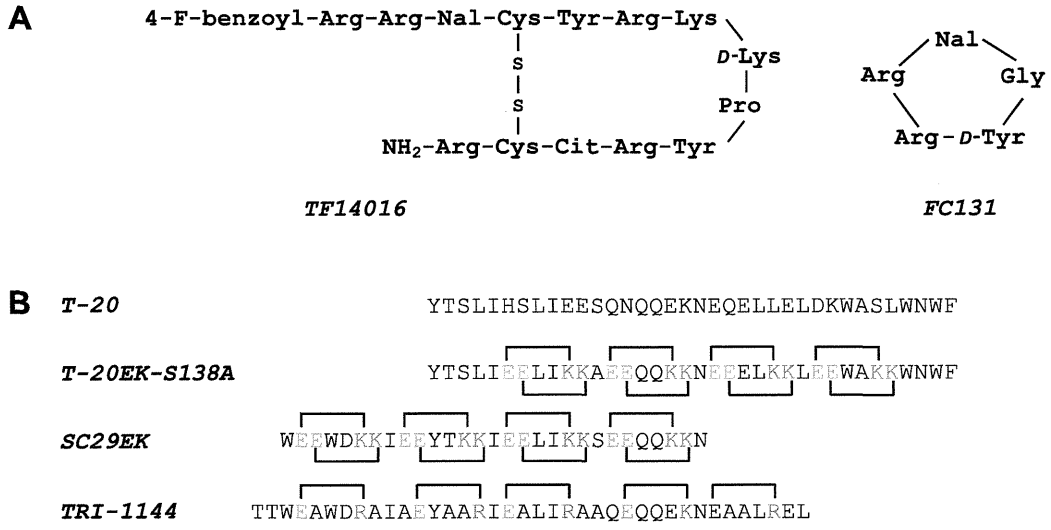

Fig. 1. Amino acid sequences of peptide-based drugs. (A) CXCR4 antagonists used in this study are shown. Nal: L-3-(2-naphthyl)alanine; Cit: L-citrulline. (B) Fusion inhibitors used are shown. T-20 is original sequenced of gp41 C-HR region. Electrostatic interactions are indicated by the linker. SC29EK and T-20EK/S138A, contain EExxKKx motif, while TRI-1144 does ExxxRxx motif. x indicates original and/or modified amino acids. Each motif creates 2 and 1 interaction(s) in each helical turn. T-20 resistance associated mutation, S138A, is introduced into T-20EK sequence (T-20EK/S138A). All peptides are N-terminally acetylated and C-terminally amidated.

with a combined rational design by the introduction of the EK motif for enhancement of α-helicity and increased affinity to mutated gp41 by S138A, a T-20 resistant associated mutation [19]. Dwyer et al. developed another fusion inhibitor, TRI-1144 (T-2635) that also exerted potent activity against T-20 resistant variants [20,21]. The amino acid sequence of TRI-1144 is also modified by substitutions with E and arginine (R), similar to the EK motif introduced into T-20EK and SC29EK.

Analyses of the efficacy and adverse effects of new drugs in animal models are important prior to their clinical application. Indeed, generally, the toxic effects, kinetics, and efficacy of new drugs are expected to be obtained by animal experiments. In the case of anti-HIV-1 drugs, the toxic effects of drug candidates can be determined by animal experiments. Furthermore, the kinetics of some drugs may be examined by some analytical methods such as liquid chromatography–mass spectrometry (LC–MS) [22] or bioimaging with labeled compounds. Unfortunately, these results may not be well-correlated with *in vivo* efficacy due to degradation and/or modification of drugs, and the detection of false positives of similar component(s) *in vivo* [23]. The efficacy of anti-HIV-1 drugs is, so far, hard to examine *in vivo* due to the lack of convenient animal infection models with low cost. One of the main obstacles to establish appropriate animal models is restricted infection of small animals with HIV-1, such as for mice, rats, and ferrets. An HIV-1 receptor-transgenic rat model has been developed for the analysis of HIV-1 infection *in vivo*; however, the levels of plasma viremia in infected rats were modest and not sustained [24,25]. Monkeys infected with simian immunodeficiency virus-HIV chimeric virus (SHIV) is the only model for the evaluation of HIV-1 replication [26], but comes at a high cost, especially for animal infection facilities. Taken together, novel rapid, simple, and sensitive HIV-1 infection models with low cost, such as those in small animals, are urgently needed to be established.

Here, we established a new system to evaluate the anti-HIV-1 activity of drugs and its kinetics in rats in addition to their toxic effects. The bioavailability of anti-HIV-1 drugs in sera was determined for the assessment of antiviral activity *in vitro*. The *in vivo* efficacy of various peptide-based entry inhibitors, such as TF14016, FC131, T-20EK/S138A, SC29EK, and TRI-1144, were assessed using this model and may be useful for the *in vivo* assessment of novel entry inhibitors.

2. Materials and methods

2.1. Drugs and cells

CXCR4 antagonists, TF14016 and FC131, and fusion inhibitors, T-20, T-20EK/S138A, SC29EK and TRI1144, were synthesized as previously described [7,9,16–18,20]. For *in vitro* drug susceptibility assays and *in vivo* administration, the test drugs were dissolved in 50% dimethyl sulfoxide (DMSO; 2 mM) and sterile water (3 or 10 mg/1.5 mL), respectively. MAGI CCR5 cells (HeLa CD4/CCR5/LTR-β-galactosidase cells) were obtained through the NIH AIDS Research and Reference Reagent Program, Division of AIDS, NIAID: from Dr. Julie Overbaugh [27–29] and were maintained in Dulbecco's modified Eagle's medium (DMEM) supplemented with 10% fetal calf serum [30].

2.2. Administration of drugs

Animal experiments were performed in the Biotechnical Center of the Japan SLC, in accordance with the institutional ethical guidelines. To examine the pharmacological kinetics in sera, rats were used for collection of sera. Drugs were used at 3 mg/1.5 mL/kg of T-20, 3 mg/1.5 mL/kg of TF14016, 10 mg/1.5 mL/kg of FC131, 10 mg/1.5 mL/kg of SC29EK, 10 mg/1.5 mL/kg of T-20EK/S138A, and 3 mg/1.5 mL/kg of TRI1144, and were intraperitoneally administrated to six groups of six male SD rats (7 weeks). Sera were then harvested 0.5, 1, 2, 4, 8, and 12 h from the administrated rat, and stored at −80 °C.

2.3. MAGI assay

The anti-HIV-1 activity of drugs in rat sera after drug administration was detected by the MAGI assay, as previously described [31]. Briefly, MAGI CCR5 cells were transferred to 96-well plates at 1×10^4 cells per well. On the following day, serially-diluted drugs or rat sera were added to cells in triplicate with HIV-1 preparations (HIV-1_{IIIB} or HIV-1_{BaL}). After 48 h, cultured cells were fixed with 1% (v/v) formaldehyde and 0.2% (v/v) glutaraldehyde in phosphate-buffered saline (PBS), and were stained with 0.4 mg/mL 5-bromo-4-chloro-3-indolyl-2-D-galactopyranoside (X-gal). Blue

cells were counted by observation under a light microscope. The 50% effective concentration was defined as the serum dilution fold or drug concentration that inhibited virus infection in 50% of the wells.

3. Results

3.1. Anti-HIV-1 activity of drugs in vitro

Prior to animal experiments, the anti-HIV-1 activity of test drugs *in vitro* was determined by the MAGI assay. HIV-1_{IIIB} and HIV-1_{BaL} were used as representative X4- and R5-tropic HIV-1 strains, respectively. TF14016 exerted most potent anti-HIV-1 activity *in vitro* compared to other inhibitors as shown in Table 1. As expected, the two CXCR4 antagonists, TF14016 and FC131, inhibited replication of only HIV-1_{IIIB}, but not HIV-1_{BaL}, which uses CCR5 for its entry. All four fusion inhibitors, T-20EK/S138A, SC29EK, TRI-1144 and T-20, comparably inhibited replication of both HIV-1_{IIIB} and HIV-1_{BaL}. Among newly developed fusion inhibitors, T-20EK/S138A showed the strongest inhibitory effect both on HIV-1_{IIIB} and HIV-1_{BaL}. Our antiviral data are similar to previous observations for TF14016 and FC131 [7–10,32], T-20EK/S138A [16], SC29EK [17], and TRI-1144 [20,21].

3.2. Anti-HIV-1 activity of CXCR4 antagonists in rat

First, we examined background anti-HIV-1 activity in four PBS-injected rat sera as negative controls. In the control rat sera, anti-HIV-1_{IIIB} and HIV-1_{BaL} activities were detected (Fig. 2). Rat sera showed antiviral activity up to the 90- and 160-fold dilution for HIV-1_{IIIB} and HIV-1_{BaL} (Fig. 2; shown as a baseline activity).

The two CXCR4 antagonists, TF14016 and FC131, were intraperitoneally injected into six rats and sera were withdrawn at the indicated time as shown in Fig. 2. Drug activities were detected up to 4 h, with peak time point at 1 h after the administration. Surprisingly, sera from two rats injected with TF14016 and four rats with FC131 also weakly showed anti-HIV-1_{BaL} activity (data not shown). However, both CXCR4 antagonists were generally effective only against HIV-1_{IIIB}.

3.3. Anti-HIV-1 activity of fusion inhibitors in rat

Anti-HIV-1_{IIIB} and anti-HIV-1_{BaL} activities were detected in four rat sera and all six rat sera, respectively, that were administered T-20. Anti-HIV-1 activity of T-20 in rats was detected up to 8 h with a peak time point 1–2 h after administration. Anti-HIV-1_{IIIB} activities were detected in sera of six rats injected with SC29EK, T-20EK/S138A, and TRI-1144, which were detected up to 3, 8, and 8 h, respectively, with serum peak levels at 1–2 h after administration. Anti-HIV-1_{BaL} activities were detected in sera with SC29EK, T-20EK/S138A, and TRI-1144 with similar extent with these for HIV-1_{IIIB}. These results indicate that in rats, intraperitoneally injected drug activities were present in sera and may exert anti-HIV-1 activity *in vivo*. Among these, TRI-1144 showed stable and relatively sustained activity.

3.4. Effect of heat inactivation

To identify component(s) for baseline anti-HIV-1 activity in rat sera, we examined heat inactivation. As expected, non-specific anti-HIV-1 activity in sera decreased in a time-dependent manner. At 1000-fold dilution of sera, non-specific activity was completely abolished (Fig. 3); unfortunately the drugs tested in the study were not heat stable and irreversible even at 56 °C (data not shown). However, when administered a physiological dose, anti-HIV-1 activity was detectable even without heat inactivation (Fig. 2). Therefore, the rat model system proved to be adequate to evaluate the efficacy of drugs.

3.5. Toxic effect of drugs in rats

All peptides tested showed no apparent lethal effect at the administered dosages, except for FC131, where one rat succumbed from unknown causes at a dose of 30 mg/kg.

4. Discussion

To develop effective and safe antiviral agents, *in vitro* screening systems are established for some viruses, while *in vivo* evaluation systems using small animals are hampered by limited infection efficiency and the need for specialized facilities. In the case of animal models for HIV-1, animal models are largely restricted [33]. In the present study, we describe the establishment of a novel evaluation system of anti-HIV-1 drugs through *in vitro* detection of anti-HIV-1 activity in the sera of rats administrated drugs using the MAGI assay. The *in vivo* efficacies of five potential entry inhibitors were evaluated. In this system, only TRI-1144 consistently showed potent and sustained activity compared with T-20. The glutamic acid–arginine (ER) modification, but not the glutamic acid–lysine (EK) modification and/or alanine substitutions to the peptide (Fig. 1), may have beneficial effects on stability and efficacy, resulting in sustained anti-HIV-1 activities. The simple and convenient *in vivo* efficacy evaluation system established in this study not only reveals whether drugs exert anti-HIV-1 activity *in vivo*, but also provides *in vivo* kinetics without the need for infectious animal facilities. Moreover, this system can be used for the evaluation of not only anti-HIV-1 drugs *in vivo*, but also of drugs against other viruses *in vivo*. Nonetheless, the sera produced by the rats can be also applied to resistant virus variants and clinical isolates resulting in a reduction of the number animal experiments required.

Other methods, such as a high performance liquid chromatography (HPLC), may provide accurate measurement of the drug concentration in sera and was performed in this study. Even after administration of FC131 at 30 mg/kg, we could only detect FC131 at the peak concentration (data not shown). In a case of small amount of agents with extremely high activity, it is possible to fail to detect by HPLC. For more sensitive detection by HPLC, further labeling, such as with radioisotopes, may be needed. In addition, HPLC analysis can detect drugs that have been modified and/or degraded by *in vivo* metabolism when they are spectrometrically indistinguishable. However, our system detects only the active

Table 1
Anti-HIV-1 activity of drugs *in vitro*.

Virus	EC_{50}[a] (nM)					
	TF14016	FC131	T-20	T-20EK/S138A	SC29EK	TRI-1144
HIV-1_{IIIB}	0.3 ± 0.0	17.4 ± 5.7	42.3 ± 7.6	2.0 ± 0.5	8.3 ± 1.3	4.6 ± 0.6
HIV-1_{BaL}	>10,000	>10,000	16.2 ± 4.9	0.4 ± 0.2	1.4 ± 0.2	0.4 ± 0.2

[a] Antiviral activity, shown as EC_{50}, was determined using the MAGI assay. Each EC_{50} represents the mean ± SD obtained from at least three independent experiments. HIV-1_{IIIB} and HIV-1_{BaL} were used as representative X4 and R5 HIV-1 strains, respectively.

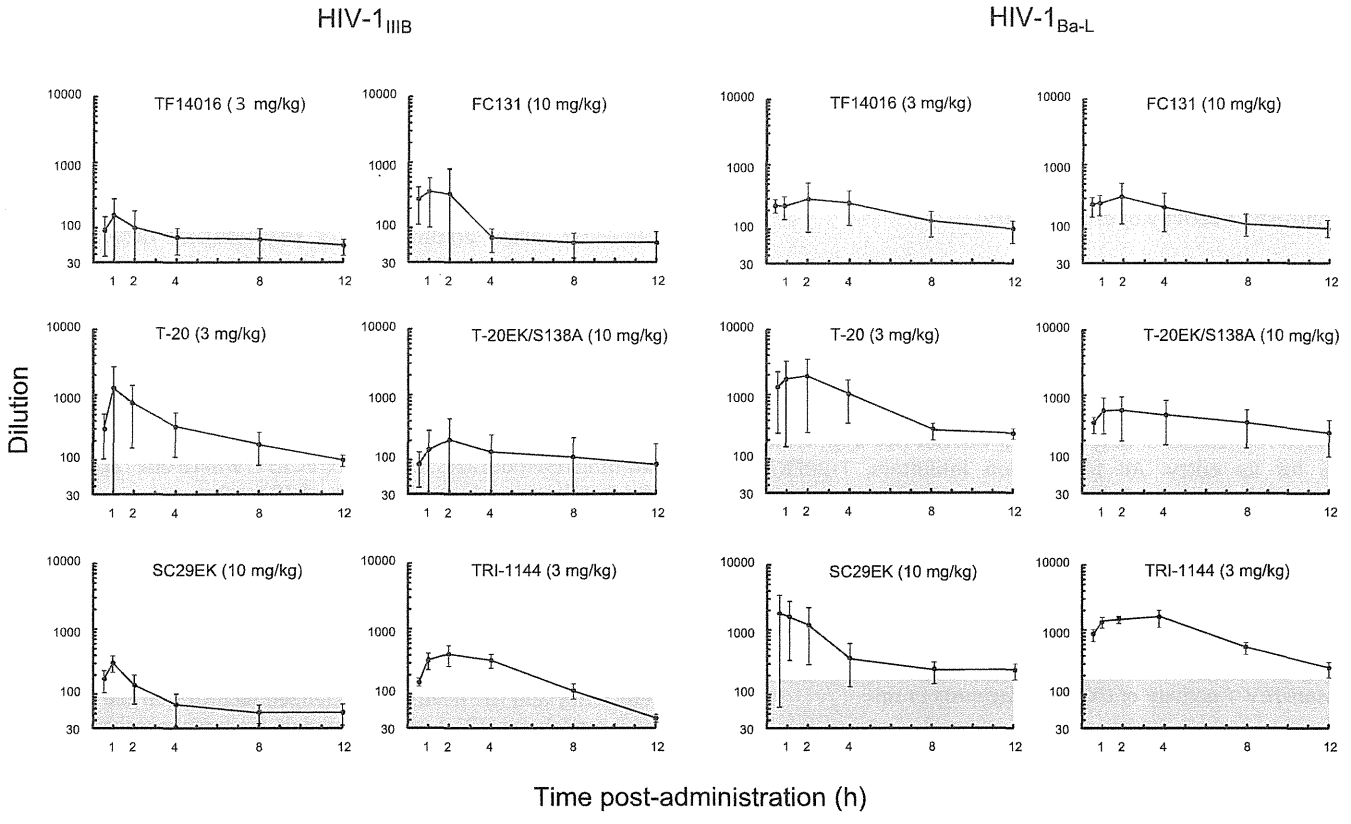

Fig. 2. Anti-HIV-1 activity of drugs *in vivo*. Six groups of six rats were administered each drug by intra-peritoneal injection and rat sera were harvested at different time points post-administration. All serum samples were analyzed by MAGI assay for 50% inhibition of infections of HIV-1_{IIIB} and HIV-1_{BaL}. This experiment was performed in triplicate for each rat. Data represent mean ± SD of from six rats. Gray shade indicates average results of age-matched rat sera as negative controls.

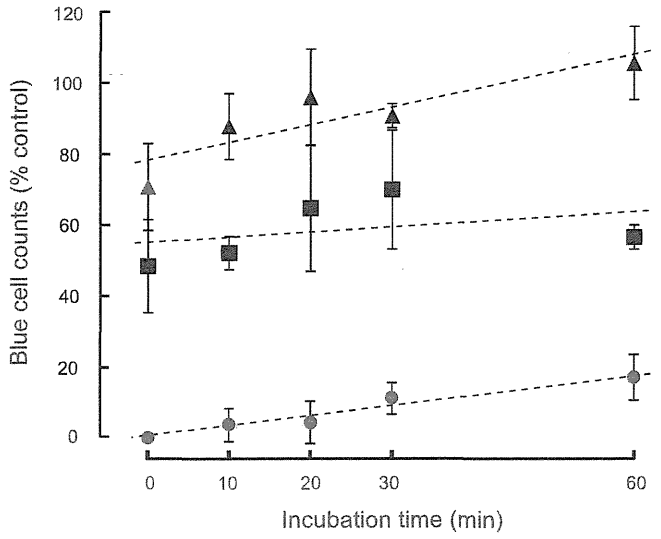

Fig. 3. Heat inactivation of sera. Rat sera without heat activation were examined using the MAGI assay. Heat inactivation was performed at 56 °C. Ten-fold dilutions of sera were resistant to heat inactivation even after 1 h inactivation (~20%). At the 1000-fold dilution, most of the inherent inhibitory effect was removed.

form of the agents, and in addition provides direct comparison of the tested drugs *in vitro* and *in vivo*, since the assay utilizes identical evaluation by the MAGI assay. In comparison, the rat *in vitro* system revealed that TRI-1144 showed strong and sustained activity compared with T-20EK/S138A and SC29EK. In this study, we only performed intraperitoneal injection that may have an effect on drug metabolism(s). Further experiments, such as subcutaneous injection, for which TF14016 shows greater efficacy [34,35], should be performed and compared with other administration roots.

The two CXCR4 antagonists analyzed in this study, TF14016 and FC131, showed moderate anti-HIV-1_{BaL} activity *in vivo*, and sera from two rats administered T-20 inhibited HIV-1 infection less efficiently (data not shown). These unexpected data might result from the relatively high background caused by non-specific inhibitory component(s) in sera. As shown in Fig. 2, sera from rats not administered drugs also showed moderate anti-HIV-1_{IIIB} and anti-HIV-1_{BaL} activities. Therefore, the development of a reagent or method for removal of background activity in rat sera may improve the accuracy and sensitivity of this *in vivo* drug efficacy evaluation method. For instance, serum albumin [36], lactoferrin [37,38], and transferrin [39] may influence HIV replication. Unfortunately, the drugs used in this study were all peptide-derived agents, therefore, heat-inactivation may reduce antiviral activity. Therefore, administration of relatively high doses of drug may be required to overcome this inhibition.

In conclusion, we established a novel, simple and rapid system for the phenotypic evaluation of anti-HIV-1 drugs in a rat model. This system may also be applicable for the analysis of other antiviral drugs for viruses that do not have an appropriate infection model in rodents, and/or useful for the initial screening, such for dosing, administration root decision and other factors, prior to actual animal infection experiments. In this system for HIV infection, TRI-1144 displayed the most potent anti-HIV-1 activity *in vivo* of the six drugs analyzed.

Acknowledgments

This work was supported by a Grant from the Ministry of Education, Culture, Sports, Science, and Technology of Japan, a Grant

for the Promotion of AIDS Research from the Ministry of Health, Labour and Welfare, a Grant for Research for Health Sciences Focusing on Drug Innovation from the Japan Health Sciences Foundation and the Science and Technology Incubation Program in Advanced Regions from the Japan Science and Technology Agency.

References

[1] E. De Clercq, Antiretroviral drugs, Curr. Opin. Pharmacol. 10 (2010) 507–515.
[2] P. Dorr, M. Westby, S. Dobbs, P. Griffin, B. Irvine, M. Macartney, J. Mori, G. Rickett, C. Smith-Burchnell, C. Napier, R. Webster, D. Armour, D. Price, B. Stammen, A. Wood, M. Perros, Maraviroc (UK-427,857), a potent, orally bioavailable, and selective small-molecule inhibitor of chemokine receptor CCR5 with broad-spectrum anti-human immunodeficiency virus type 1 activity, Antimicrob. Agents Chemother. 49 (2005) 4721–4732.
[3] C.T. Wild, D.C. Shugars, T.K. Greenwell, C.B. McDanal, T.J. Matthews, Peptides corresponding to a predictive alpha-helical domain of human immunodeficiency virus type 1 gp41 are potent inhibitors of virus infection, Proc. Natl. Acad. Sci. USA 91 (1994) 9770–9774.
[4] G. Fatkenheuer, A.L. Pozniak, M.A. Johnson, A. Plettenberg, S. Staszewski, A.I. Hoepelman, M.S. Saag, F.D. Goebel, J.K. Rockstroh, B.J. Dezube, T.M. Jenkins, C. Medhurst, J.F. Sullivan, C. Ridgway, S. Abel, I.T. James, M. Youle, E. van der Ryst, Efficacy of short-term monotherapy with maraviroc, a new CCR5 antagonist, in patients infected with HIV-1, Nat. Med. 11 (2005) 1170–1172.
[5] J.P. Lalezari, K. Henry, M. O'Hearn, J.S. Montaner, P.J. Piliero, B. Trottier, S. Walmsley, C. Cohen, D.R. Kuritzkes, J.J. Eron Jr., J. Chung, R. DeMasi, L. Donatacci, C. Drobnes, J. Delehanty, M. Salgo, Enfuvirtide, an HIV-1 fusion inhibitor, for drug-resistant HIV infection in North and South America, N. Engl. J. Med. 348 (2003) 2175–2185.
[6] Y. Feng, C.C. Broder, P.E. Kennedy, E.A. Berger, HIV-1 entry cofactor: functional cDNA cloning of a seven-transmembrane, G protein-coupled receptor, Science 272 (1996) 872–877.
[7] H. Tamamura, A. Omagari, S. Oishi, T. Kanamoto, N. Yamamoto, S.C. Peiper, H. Nakashima, A. Otaka, N. Fujii, Pharmacophore identification of a specific CXCR4 inhibitor, T140, leads to development of effective anti-HIV agents with very high selectivity indexes, Bioorg. Med. Chem. Lett. 10 (2000) 2633–2637.
[8] H. Tamamura, Y. Xu, T. Hattori, X. Zhang, R. Arakaki, K. Kanbara, A. Omagari, A. Otaka, T. Ibuka, N. Yamamoto, H. Nakashima, N. Fujii, A low-molecular-weight inhibitor against the chemokine receptor CXCR4: a strong anti-HIV peptide T140, Biochem. Biophys. Res. Commun. 253 (1998) 877–882.
[9] N. Fujii, S. Oishi, K. Hiramatsu, T. Araki, S. Ueda, H. Tamamura, A. Otaka, S. Kusano, S. Terakubo, H. Nakashima, J.A. Broach, J.O. Trent, Z.X. Wang, S.C. Peiper, Molecular-size reduction of a potent CXCR4-chemokine antagonist using orthogonal combination of conformation- and sequence-based libraries, Angew. Chem. Int. Ed. Engl. 42 (2003) 3251–3253.
[10] H. Tamamura, K. Hiramatsu, M. Mizumoto, S. Ueda, S. Kusano, S. Terakubo, M. Akamatsu, N. Yamamoto, J.O. Trent, Z. Wang, S.C. Peiper, H. Nakashima, A. Otaka, N. Fujii, Enhancement of the T140-based pharmacophores leads to the development of more potent and bio-stable CXCR4 antagonists, Org. Biomol. Chem. 1 (2003) 3663–3669.
[11] J.P. Lalezari, K. Henry, M. O'Hearn, J.S. Montaner, P.J. Piliero, B. Trottier, S. Walmsley, C. Cohen, D.R. Kuritzkes, J.J. Eron, J. Chung, R. DeMasi, L. Donatacci, C. Drobnes, J. Delehanty, M. Salgo, T.S. Group, Enfuvirtide, an HIV-1 fusion inhibitor, for drug-resistant HIV infection in North and South America, N. Engl. J. Med. 348 (2003) 2175–2185.
[12] A. Lazzarin, B. Clotet, D. Cooper, J. Reynes, K. Arasteh, M. Nelson, C. Katlama, H.J. Stellbrink, J.F. Delfraissy, J. Lange, L. Huson, R. DeMasi, C. Wat, J. Delehanty, C. Drobnes, M. Salgo, T.S. Group, Efficacy of enfuvirtide in patients infected with drug-resistant HIV-1 in Europe and Australia, N. Engl. J. Med. 348 (2003) 2186–2195.
[13] B. Labrosse, L. Morand-Joubert, A. Goubard, S. Rochas, J.L. Labernardière, J. Pacanowski, J.L. Meynard, A.J. Hance, F. Clavel, F. Mammano, Role of the envelope genetic context in the development of enfuvirtide resistance in human immunodeficiency virus type 1-infected patients, J. Virol. 80 (2006) 8807–8819.
[14] E. Poveda, B. Rodés, C. Toro, L. Martín-Carbonero, J. Gonzalez-Lahoz, V. Soriano, Evolution of the gp41 env region in HIV-infected patients receiving T-20, a fusion inhibitor, AIDS 16 (2002) 1959–1961.
[15] B. Zöllner, H.H. Feucht, M. Schröter, P. Schäfer, A. Plettenberg, A. Stoehr, R. Laufs, Primary genotypic resistance of HIV-1 to the fusion inhibitor T-20 in long-term infected patients, AIDS 15 (2001) 935–936.
[16] S. Oishi, S. Ito, H. Nishikawa, K. Watanabe, M. Tanaka, H. Ohno, K. Izumi, Y. Sakagami, E. Kodama, M. Matsuoka, N. Fujii, Design of a novel HIV-1 fusion inhibitor that displays a minimal interface for binding affinity, J. Med. Chem. 51 (2008) 388–391.
[17] T. Naito, K. Izumi, E. Kodama, Y. Sakagami, K. Kajiwara, H. Nishikawa, K. Watanabe, S.G. Sarafianos, S. Oishi, N. Fujii, M. Matsuoka, SC29EK, a peptide fusion inhibitor with enhanced alpha-helicity, inhibits replication of human immunodeficiency virus type 1 mutants resistant to enfuvirtide, Antimicrob. Agents Chemother. 53 (2009) 1013–1018.
[18] H. Nishikawa, S. Oishi, M. Fujita, K. Watanabe, R. Tokiwa, H. Ohno, E. Kodama, K. Izumi, K. Kajiwara, T. Naitoh, M. Matsuoka, A. Otaka, N. Fujii, Identification of minimal sequence for HIV-1 fusion inhibitors, Bioorg. Med. Chem. 16 (2008) 9184–9187.
[19] K. Izumi, E. Kodama, K. Shimura, Y. Sakagami, K. Watanabe, S. Ito, T. Watabe, Y. Terakawa, H. Nishikawa, S.G. Sarafianos, K. Kitaura, S. Oishi, N. Fujii, M. Matsuoka, Design of peptide-based inhibitors for human immunodeficiency virus type 1 strains resistant to T-20, J. Biol. Chem. (2009) 4914–4920.
[20] D.K. Davison, R.J. Medinas, S.M. Mosier, T.S. Bowling, M.K. Delmedico, J.J. Dwyer, N. Cammack, M.L. Greenberg, New fusion inhibitor peptides, TRI-999 and TRI-1144, are potent inhibitors of enfuvirtide and T-1249 resistant isolates. in: Program and Abstracts of the 16 th International AIDS Conference, August 13 -18, 2006,Toronto, Canada, Abstract THPE0021.
[21] J.J. Dwyer, K.L. Wilson, D.K. Davison, S.A. Freel, J.E. Seedorff, S.A. Wring, N.A. Tvermoes, T.J. Matthews, M.L. Greenberg, M.K. Delmedico, Design of helical, oligomeric HIV-1 fusion inhibitor peptides with potent activity against enfuvirtide-resistant virus, Proc. Natl. Acad. Sci. USA 104 (2007) 12772–12777.
[22] E.N. Fung, Z. Cai, T.C. Burnette, A.K. Sinhababu, Simultaneous determination of Ziagen and its phosphorylated metabolites by ion-pairing high-performance liquid chromatography–tandem mass spectrometry, J. Chromatogr. B Biomed. Sci. Appl. 754 (2001) 285–295.
[23] Z. Cai, E.N. Fung, A.K. Sinhababu, Capillary electrophoresis-ion trap mass spectrometry analysis of Ziagen and its phosphorylated metabolites, Electrophoresis 24 (2003) 3160–3164.
[24] C. Goffinet, I. Allespach, O.T. Keppler, HIV-susceptible transgenic rats allow rapid preclinical testing of antiviral compounds targeting virus entry or reverse transcription, Proc. Natl. Acad. Sci. USA 104 (2007) 1015–1020.
[25] O.T. Keppler, F.J. Welte, T.A. Ngo, P.S. Chin, K.S. Patton, C.L. Tsou, N.W. Abbey, M.E. Sharkey, R.M. Grant, Y. You, J.D. Scarborough, W. Ellmeier, D.R. Littman, M. Stevenson, I.F. Charo, B.G. Herndier, R.F. Speck, M.A. Goldsmith, Progress toward a human CD4/CCR5 transgenic rat model for de novo infection by human immunodeficiency virus type 1, J. Exp. Med. 195 (2002) 719–736.
[26] R. Shibata, A. Adachi, SIV/HIV recombinants and their use in studying biological properties, AIDS Res. Hum. Retroviruses 8 (1992) 403–409.
[27] B. Chackerian, E.M. Long, P.A. Luciw, J. Overbaugh, Human immunodeficiency virus type 1 coreceptors participate in postentry stages in the virus replication cycle and function in simian immunodeficiency virus infection, J. Virol. 71 (1997) 3932–3939.
[28] J. Kimpton, M. Emerman, Detection of replication-competent and pseudotyped human immunodeficiency virus with a sensitive cell line on the basis of activation of an integrated beta-galactosidase gene, J. Virol. 66 (1992) 2232–2239.
[29] H. Deng, R. Liu, W. Ellmeier, S. Choe, D. Unutmaz, M. Burkhart, P. Di Marzio, S. Marmon, R.E. Sutton, C.M. Hill, C.B. Davis, S.C. Peiper, T.J. Schall, D.R. Littman, N.R. Landau, Identification of a major co-receptor for primary isolates of HIV-1, Nature 381 (1996) 661–666.
[30] E.I. Kodama, S. Kohgo, K. Kitano, H. Machida, H. Gatanaga, S. Shigeta, M. Matsuoka, H. Ohrui, H. Mitsuya, 4′-Ethynyl nucleoside analogs: potent inhibitors of multidrug-resistant human immunodeficiency virus variants *in vitro*, Antimicrob. Agents Chemother. 45 (2001) 1539–1546.
[31] D. Nameki, E. Kodama, M. Ikeuchi, N. Mabuchi, A. Otaka, H. Tamamura, M. Ohno, N. Fujii, M. Matsuoka, Mutations conferring resistance to human immunodeficiency virus type 1 fusion inhibitors are restricted by gp41 and Rev-responsive element functions, J. Virol. 79 (2005) 764–770.
[32] H. Tamamura, K. Hiramatsu, S. Ueda, Z. Wang, S. Kusano, S. Terakubo, J.O. Trent, S.C. Peiper, N. Yamamoto, H. Nakashima, A. Otaka, N. Fujii, Stereoselective synthesis of [L-Arg-L/D-3-(2-naphthyl)alanine]-type (E)-alkene dipeptide isosteres and its application to the synthesis and biological evaluation of pseudopeptide analogues of the CXCR4 antagonist FC131, J. Med. Chem. 48 (2005) 380–391.
[33] K.K. Van Rompay, Evaluation of antiretrovirals in animal models of HIV infection, Antiviral Res. 85 (2010) 159–175.
[34] K. Nishizawa, H. Nishiyama, Y. Matsui, T. Kobayashi, R. Saito, H. Kotani, H. Masutani, S. Oishi, Y. Toda, N. Fujii, J. Yodoi, O. Ogawa, Thioredoxin-interacting protein suppresses bladder carcinogenesis, Carcinogenesis 32 (2011) 1459–1466.
[35] T. Kitaori, H. Ito, E.M. Schwarz, R. Tsutsumi, H. Yoshitomi, S. Oishi, M. Nakano, N. Fujii, T. Nagasawa, T. Nakamura, Stromal cell-derived factor 1/CXCR4 signaling is critical for the recruitment of mesenchymal stem cells to the fracture site during skeletal repair in a mouse model, Arthritis Rheum. 60 (2009) 813–823.
[36] M.E. Kuipers, J.G. Huisman, P.J. Swart, M.P. de Béthune, R. Pauwels, H. Schuitemaker, E. De Clercq, D.K. Meijer, Mechanism of anti-HIV activity of negatively charged albumins: biomolecular interaction with the HIV-1 envelope protein gp120, J. Acquir. Immune Defic. Syndr. Hum. Retrovirol. 11 (1996) 419–429.
[37] F. Groot, T.B. Geijtenbeek, R.W. Sanders, C.E. Baldwin, M. Sanchez-Hernandez, R. Floris, Y. van Kooyk, E.C. de Jong, B. Berkhout, Lactoferrin prevents dendritic cell-mediated human immunodeficiency virus type 1 transmission by blocking the DC-SIGN–gp120 interaction, J. Virol. 79 (2005) 3009–3015.
[38] M.C. Harmsen, P.J. Swart, M.P. de Béthune, R. Pauwels, E. De Clercq, T.H. The, D.K. Meijer, Antiviral effects of plasma and milk proteins: lactoferrin shows potent activity against both human immunodeficiency virus and human cytomegalovirus replication *in vitro*, J. Infect. Dis. 172 (1995) 380–388.
[39] H. Drakesmith, A. Prentice, Viral infection and iron metabolism, Nat. Rev. Microbiol. 6 (2008) 541–552.

THE JOURNAL OF BIOLOGICAL CHEMISTRY VOL. 287, NO. 35, pp. 29988–29999, August 24, 2012

HIV-1 Reverse Transcriptase (RT) Polymorphism 172K Suppresses the Effect of Clinically Relevant Drug Resistance Mutations to Both Nucleoside and Non-nucleoside RT Inhibitors*[S]

Received for publication, February 8, 2012, and in revised form, April 24, 2012 Published, JBC Papers in Press, July 2, 2012, DOI 10.1074/jbc.M112.351551

Atsuko Hachiya[‡§], Bruno Marchand[‡1], Karen A. Kirby[‡], Eleftherios Michailidis[‡], Xiongying Tu[¶], Krzysztof Palczewski[¶], Yee Tsuey Ong[‡], Zhe Li[‡‖], Daniel T. Griffin[‡], Matthew M. Schuckmann[‡], Junko Tanuma[§], Shinichi Oka[§], Kamalendra Singh[‡], Eiichi N. Kodama[**], and Stefan G. Sarafianos[‡‖2]

From the [‡]Christopher S. Bond Life Sciences Center, Department of Molecular Microbiology and Immunology, University of Missouri School of Medicine, Columbia, Missouri 65211, the [§]AIDS Clinical Center, National Center for Global Health and Medicine, Tokyo 162-8655, Japan, [¶]Case Western University, Cleveland, Ohio 44106, the [**]Division of Emerging Infectious Diseases, Tohoku University School of Medicine, Sendai 980-8575, Japan, and the [‖]Department of Biochemistry, University of Missouri, Columbia, Missouri 65211

Background: The effect of HIV polymorphisms in drug resistance is unknown.
Results: RT polymorphism 172K suppresses resistance to nucleoside (NRTIs) and non-nucleoside RT inhibitors (NNRTIs) by decreasing DNA binding and restoring NNRTI binding.
Conclusion: 172K is the first HIV polymorphism suppressing resistance to diverse inhibitors.
Significance: Results provide new insights into interactions between the polymerase active site and NNRTI-binding sites.

Polymorphisms have poorly understood effects on drug susceptibility and may affect the outcome of HIV treatment. We have discovered that an HIV-1 reverse transcriptase (RT) polymorphism (RT_{172K}) is present in clinical samples and in widely used laboratory strains (BH10), and it profoundly affects HIV-1 susceptibility to both nucleoside (NRTIs) and non-nucleoside RT inhibitors (NNRTIs) when combined with certain mutations. Polymorphism 172K significantly suppressed zidovudine resistance caused by excision (*e.g.* thymidine-associated mutations) and not by discrimination mechanism mutations (*e.g.* Q151M complex). Moreover, it attenuated resistance to nevirapine or efavirenz imparted by NNRTI mutations. Although 172K favored RT-DNA binding at an excisable pre-translocation conformation, it decreased excision by thymidine-associated mutation-containing RT. 172K affected DNA handling and decreased RT processivity without significantly affecting the k_{cat}/K_m values for dNTP. Surface plasmon resonance experiments revealed that RT_{172K} decreased DNA binding by increasing the dissociation rate. Hence, the increased zidovudine susceptibility of RT_{172K} results from its increased dissociation from the chain-terminated DNA and reduced primer unblocking. We solved a high resolution (2.15 Å) crystal structure of RT mutated at 172 and compared crystal structures of RT_{172R} and RT_{172K} bound to NNRTIs or DNA/dNTP. Our structural analyses highlight differences in the interactions between α-helix E (where 172 resides) and the active site β9-strand that involve the YMDD loop and the NNRTI binding pocket. Such changes may increase dissociation of DNA, thus suppressing excision-based NRTI resistance and also offset the effect of NNRTI resistance mutations thereby restoring NNRTI binding.

Human immunodeficiency virus type 1 (HIV-1) reverse transcriptase (RT) has been a major target of antiviral therapies. There are two classes of approved RT drugs as follows: nucleos(t)ide RT inhibitors (NRTI)[3] and non-nucleoside RT inhibitors (NNRTI). NRTIs are incorporated in the nascent DNA chain during reverse transcription and block further DNA synthesis by acting as chain terminators because they lack a 3′-hydroxyl group required for formation of a phosphodiester bond (1–3). NNRTIs are noncompetitive allosteric inhibitors that decrease the rate of nucleotide incorporation by binding to a hydrophobic pocket adjacent to the catalytic site (4–6).

* This work was supported, in whole or in part, by National Institutes of Health Research Grants AI094715, AI076119, AI079801, and AI074389 (to S. G. S.). This work was also supported by a grant for the promotion of AIDS research from the Ministry of Health, Labor, and Welfare (to E. K., A. H., and S. O.), by a grant for the Japan Initiative for Global Research Network on Infectious Diseases from the Ministry of Education, Culture, Sports, Science, and Technology (to J. T. and S. O.), and by a grant for Bilateral International Collaborative R&D Program from the Korea Food and Drug Administration and the Ministry of Knowledge and Economy (to S. G. S.).
[S] This article contains supplemental Figs. 1 and 2 and Tables 1–4.
The atomic coordinates and structure factors (code 4DG1) have been deposited in the Protein Data Bank, Research Collaboratory for Structural Bioinformatics, Rutgers University, New Brunswick, NJ (http://www.rcsb.org/).
[1] Recipient of an American Foundation for AIDS Research Mathilde Krim fellowship and a Canadian Institutes of Health Research fellowship.
[2] To whom correspondence should be addressed: 471d Christopher S. Bond Life Sciences Center, 1201 E. Rollins St., Columbia, MO 65211. Tel.: 573-882-4338; E-mail: sarafianoss@missouri.edu.

[3] The abbreviations used are: NRTI, nucleoside RT inhibitor; NNRTI, non-nucleoside RT inhibitor; TAM, thymidine-associated mutation; AZT, zidovudine; NVP, nevirapine; EFV, efavirenz; d4T, stavudine; ddI, didanosine; TDF, tenofovir; ABC, abacavir; AZT-MP, AZT-monophosphate; SPR, surface plasmon resonance; PDB, Protein Data Bank; BisTris, 2-[bis(2-hydroxyethyl)amino]-2-(hydroxymethyl)propane-1,3-diol; RTI, RT inhibitor; RVT, D-2′,3′-didehydro-2′,3′-dideoxy-5-fluorocytidine; TP, triphosphate; 3TC, lamivudine; T/P, template/primer.

There are two main mechanisms for resistance to NRTIs. In the first mechanism, RT preferentially decreases incorporation of NRTI-triphosphates (TPs), while retaining the ability to use natural nucleotide substrates. This type of resistance is typically imparted by mutations close to the nucleotide-binding site of RT. For instance, K65R, L74V, and Q151M decrease the incorporation rate of NRTI-TPs (7–10), whereas M184V sterically hinders productive binding of lamivudine (3TC)-TPs at the dNTP-binding site (11). The second mechanism of NRTI resistance involves unblocking of the NRTI-terminated primers by an excision activity that uses ATP (12–15). This excision activity is enhanced (12) in the presence of mutations such as M41L, D67N, K70R, L210W, T215Y/F, and K219Q/E (thymidine-associated mutations, TAMs), which are selected during zidovudine (AZT) or stavudine (d4T) therapy (16, 17). It has been reported by several groups, including ours, that other RT mutations located far from the polymerase active site at the connection subdomain (E312Q, G335C/D, N348I, A360I/V, V365I, and A376S) confer resistance to NRTIs and/or NNRTIs (18–25). It has been proposed that reduction of RNase H cleavage caused by connection subdomain mutations contributes to NRTI resistance by providing more time for RT to carry out excision and resume productive DNA synthesis (24–28).

There are several examples of RT mutations that cause resistance to one drug and affect the emergence of resistance mutations to another drug. For example, treatment of patients with AZT and 3TC combinations often results in the emergence of the 3TC resistance mutation M184V, but it also delays acquisition of TAMs (29, 30). In addition, appearance of the primary didanosine (ddI) resistance mutation L74V precludes AZT resistance conferred by TAMs (29, 31). Conversely, appearance of the first TAM (T215Y) during AZT and ddI combination therapy suppresses emergence of L74V (32). Tenofovir (TDF) resistance mutation K65R has a strong negative association with TAMs but not with other NRTI mutations, including Q151M complex (Q151Mc) (33). The bidirectional phenotypic antagonism between K65R and TAMs suppresses not only AZT resistance conferred by TAMs but also abacavir (ABC), ddI, and TDF resistance conferred by K65R (33, 34). Moreover, NNRTI resistance mutations L100I and Y181C are also antagonistic to AZT resistance by TAMs (32, 35, 36) because they reduce ATP-mediated unblocking of AZT-terminated primers (34, 35, 37–39). Such antagonistic interactions between resistance mutations impart significant clinical benefits. Hence, to optimize clinical decisions, it is very important to understand how mutations may affect the phenotype of known drug resistance mutations.

It is known that certain HIV-1 RT polymorphisms beyond the currently known canonical NRTI resistance mutations contribute to the evolution of NRTI resistance (40). Polymorphisms T39A, K43E/Q, K122E, E203K, and H208Y lead to TAM-1 (M41L/L210W/T215Y), whereas D218E leads to TAM-2 (D67N/K70R/T215F/K219Q). Moreover, an extensive cross-sectional study has demonstrated that some HIV-1 RT polymorphisms strongly correlate with virological failure of NRTI-based treatments (41).

Although codon 172 of HIV-1 RT is usually an arginine (172R), a lysine (172K) polymorphism is also found in clinical samples (up to 1.0%, as reported at the HIV Drug Resistance Database) and in the BH10 laboratory strain, which is very commonly used in drug resistance studies. This study uses virological, biochemical, and structural tools to reveal the effect of 172K on NRTI NNRTI. We report that 172K significantly suppresses resistance to both NRTIs and NNRTIs, and we propose specific biochemical mechanisms for these effects.

EXPERIMENTAL PROCEDURES

Antiviral Agents—AZT, d4T, and ddI were purchased from Sigma. 3TC and TDF were purchased from Moravek Biochemicals, Inc. (Brea, CA). ABC, nevirapine (NVP), and efavirenz (EFV) were provided by the AIDS Research and Reference Reagent Program (National Institutes of Health).

Cells and Viruses—COS-7 and MAGIC-5 cells (CCR5 transduced HeLa-CD4/LTR-β-gal cells) were maintained in Dulbecco's modified Eagle's medium supplemented with 10% fetal calf serum, 100 unit/ml penicillin, and 100 μg/ml streptomycin and used for transfection and antiviral assays, respectively, as described previously (42).

RT mutations were introduced by site-directed mutagenesis as described previously (20, 43). The pNL101 HIV-1 infectious clone was provided by Dr. K.-T. Jeang (National Institutes of Health, Bethesda) and used for generating recombinant HIV-1 clones. Wild-type HIV-1 (HIV-1_{WT}) was constructed by replacing the *pol*-coding region of pNL101 (nucleotides position; nucleotide 2006 of ApaI site to 5785 of SalI site of pNL101) with HIV-1 BH10 strain. We introduced a silent mutation at nucleotide 4232 (TTTAGA to TCTAGA) of the *pol*-coding region to generate a unique XbaI site. The desired mutations were introduced into the XmaI-XbaI region (1643 bp), which encodes nucleotides 2590–4232 of pNL101. This cassette was cloned into the respective sites of pBluescript vector (Stratagene) and introduced mutation(s) using an oligonucleotide-based site-directed mutagenesis method. After mutagenesis, the XmaI-XbaI cassettes were inserted back into pNL101 and confirmed by sequencing. Viral stocks were obtained by transfection of each molecular clone into COS-7 cells, harvested, and stored at −80 °C until use.

Drug Susceptibility Assays—Single replication cycle drug susceptibility assays were performed in triplicates using MAGIC-5 cells as described previously (42). Briefly, MAGIC-5 cells were infected with diluted virus stock at 100 blue forming units in the presence of increasing concentrations of RTIs, cultured for 48 h, fixed, and stained with 5-bromo-4-chloro-3-indolyl-D-galactopyranoside (X-gal). The stained cells were counted under a light microscope. The susceptibility of RTIs was calculated as the concentration that reduces blue forming units (infection) by 50% (50% effective concentration [EC_{50}]).

Enzymes and Nucleic Acid Substrates—Mutant RTs were generated through site-directed mutagenesis and replaced into the pRT dual vector using restriction sites PpuMI and SacI for the p51 subunit and SacII and AvrII for the p66 subunit. Heterodimeric HIV-1 RTs (p66 and p51) were expressed in *Escherichia coli*, BL21, and purified as described previously (44, 45).

For the primer extension and RT processivity assays we used an 18-nucleotide DNA primer fluorescently labeled with Cy3 at the 5′ end (P_{18long}; 5′-Cy3 GTC CCT GTT CGG GCG CCA-3′)

annealed to a 100-nucleotide DNA template (T_{100}; 5′-TAG TGT GTG CCC GTC TGT TGT GTG ACT CTG GTA ACT AGA GAT CCC TCA GAC CCT TTT AGT CAG TGT GGA AAA TCT CTA GCA GTG GCG CCC GAA CAG GGA C-3′) as described previously (44–46). For steady state kinetics, an 18-nucleotide DNA primer 5′-labeled with Cy3 (P_{18}; 5′-Cy3 GTC ACT GTT CGA GCA CCA-3′) annealed to a 31-nucleotide DNA template (T_{31}; 5′-CCA TAG ATA GCA TTG GTG CTC GAA CAG TGA C-3′). For the site-specific Fe^{2+} footprinting assay, we used a 30-nucleotide DNA primer (P_{30}; 5′-TCT ACA CTG ATT GTC ACT GTT CGA GCA CCA-3′) annealed to a 43-nucleotide DNA template 5′-labeled with Cy3 (T_{43}; 5′-Cy3 CCA TAG CTA GCT ATG GTG CTC GAA CAG TGA CAA TCA GTG TAG A-3′).

Primer Extension Assays—Primer extension assays were performed in the presence of AZT-TP or NVP as we described previously (44). Reactions contained 50 nM T_{100}/5′-Cy3-P_{18long} mixed with 120 nM RT (in experiments with AZT-TP) or 80 nM RT (in experiments with NVP) in a buffer containing 50 mM Tris-HCl, pH 7.8, and 50 mM NaCl, 1 μM of each dNTP, 0.5 mM EDTA, and varying concentrations of AZT-TP or NVP. In NVP-containing reactions, RT was preincubated with template/primer (T/P) and inhibitor at 37 °C for 5 min. DNA synthesis was initiated by the addition of 10 mM $MgCl_2$. Reactions were terminated after 40 min (AZT-TP) or 30 min (NVP) by adding an equal volume of 100% formamide-containing traces of bromphenol blue. Extension products were loaded on a 7 M urea, 15% polyacrylamide gel. The gels were scanned using a FLA-5000 PhosphorImager (FujiFilm, Stamford, CT). The amounts of full-length extended and unextended products were quantified by densitometry using MultiGauge, and the results were plotted using GraphPad Prism 4 (GraphPad Software Inc.).

Site-specific Fe^{2+} Footprinting Assays—Site-specific Fe^{2+} footprinting assays were performed using 5′-Cy3-labeled DNA templates as described previously (46, 47). Briefly, 100 nM 5′-Cy3-T_{43}/P_{30} was incubated at 37 °C with HIV-1 RT (600 nM) for 30 min in a buffer containing 120 mM sodium cacodylate, pH 7.0, 20 mM NaCl, 6 mM $MgCl_2$, and 10 μM AZT-TP to allow quantitative chain termination. Complexes were preincubated for 7 min with increasing concentrations of the next nucleotide (dATP), and 1 mM ammonium iron sulfate was added. The reactions were quenched after 5 min with 30 μl of formamide containing bromphenol blue. The products were resolved with gel electrophoresis in 7 M urea, 15% polyacrylamide gels.

Surface Plasmon Resonance Assay—We used surface plasmon resonance (SPR) to measure the binding affinity of RT_{172K} and RT_{172R} to double-stranded DNA. Experiments were performed on a Biacore T100 instrument (GE Healthcare). To prepare the sensor chip surface, we used the 5′-biotin-T_{d37}/P_{d25} (5′-biotin-TAG ATC AGT CAT GCT CCG CGC CCG AAC AGG GAC TGT G-3′, annealed to P_{d25} 5′-CAC AGT CCC TGT TCG GGC GCG GAG C-3′). Approximately 100 resonance units of this DNA duplex were bound in a channel of a streptavidin-coated sensor chips (Series S Sensor Chip SA) by flowing 0.1 μM DNA (flow rate 10 μl/min) in 50 mM Tris, pH 7.8, 50 mM NaCl. The binding constants were determined as follows: RT binding was observed by flowing solutions containing increasing concentrations of the enzyme (0.5, 1, 2, 4, 7.5, 10, 15, and 20 nM) in 50 mM Tris, pH 7.8, 60 mM KCl, 10 mM $MgCl_2$ in sample and background channels at 30 μl/min. The background traces were subtracted from the traces of the corresponding samples to obtain the binding signal of RT. This signal was analyzed using the Biacore T100 Evaluation software to determine K_D, k_{on}, and k_{off} values.

Enzyme Processivity Assays—Processivity assays were performed in the presence of a heparin trap to ensure that each synthesized DNA molecule resulted from a single processive cycle. Twenty nanomolar T_{100}/5′-Cy3-P_{18long} was preincubated with 500 nM RT at 37 °C in a buffer containing 50 mM Tris-HCl, pH 7.8, 50 mM NaCl, 50 μM of each dNTP, and 0.1 mM EDTA for 5 min. DNA synthesis was initiated by the addition of 10 mM $MgCl_2$ and 2 mg/ml heparin. Reactions were terminated after 0, 15, and 90 min by adding an equal volume of 100% formamide containing traces of bromphenol blue. Extension products were loaded on a 7 M urea, 15% polyacrylamide gel, quantified, and analyzed as described above.

Steady State Kinetics—Steady state parameters K_m and k_{cat} for incorporation of a nucleotide were determined using a single nucleotide incorporation gel-based assay. Reactions with RT_{172K} and RT_{172R} were carried out in 50 mM Tris-HCl, pH 7.8, 50 mM NaCl, 6 mM $MgCl_2$, 100 nM T/P, 10 nM RT, respectively, and varying concentrations of dNTP in a final volume of 10 μl. The reactions for HIV-1 RT were carried out in Reaction Buffer with 100 nM T_{31}/5′-Cy3-P_{18}. Reactions were stopped after 1 min at 37 °C, and the products were resolved and quantified as described above. K_m and k_{cat} values were determined graphically by using the Michaelis-Menten equation.

Crystallization of RT—RT with mutations K172A and K173A was prepared as described by Bauman *et al.* (48). These changes have been reported to strongly improve diffraction of RT. The enzyme was crystallized by the hanging drop vapor diffusion technique at 4 °C. The well solution contained 50 mM BisTris, pH 6.8, 100 mM ammonium sulfate, 10% glycerol, and 12% PEG 8000. Two μl of the well solution was mixed with 2 μl of RT (30 mg/ml) containing 10 mM $MgCl_2$, 10 mM Tris, pH 7.8, and 25 mM NaCl. The drop was equilibrated against the well solution by hanging a coverslip over the sealed well. The drops were streak-seeded with crushed RT crystals after 7 days of incubation. Crystals were obtained 7–14 days after the drops were seeded. Single crystals were soaked in cryoprotectant solution containing the well solution supplemented with 22.5% ethylene glycol for 15–60 s and frozen in liquid nitrogen.

Structure Solution—Diffraction datasets were collected at the Advanced Light Source Synchrotron beamline 4.2.2. The data were processed to 2.15 Å using MOSFLM (49) (supplemental Table 1). Molecular replacement phasing was performed using Phaser (50) and a previously solved RT structure as a model (Protein Data Bank (PDB) code 3KLI). The final model was obtained after cycles of iterative model building in COOT (51) and restrained refinement with CNS (52) and REFMAC (53). Final statistics for data processing and structure refinement are listed in supplemental Table 1. Coordinates and structure factors for the crystal structure were deposited to the PDB (PDB code 4DG1).

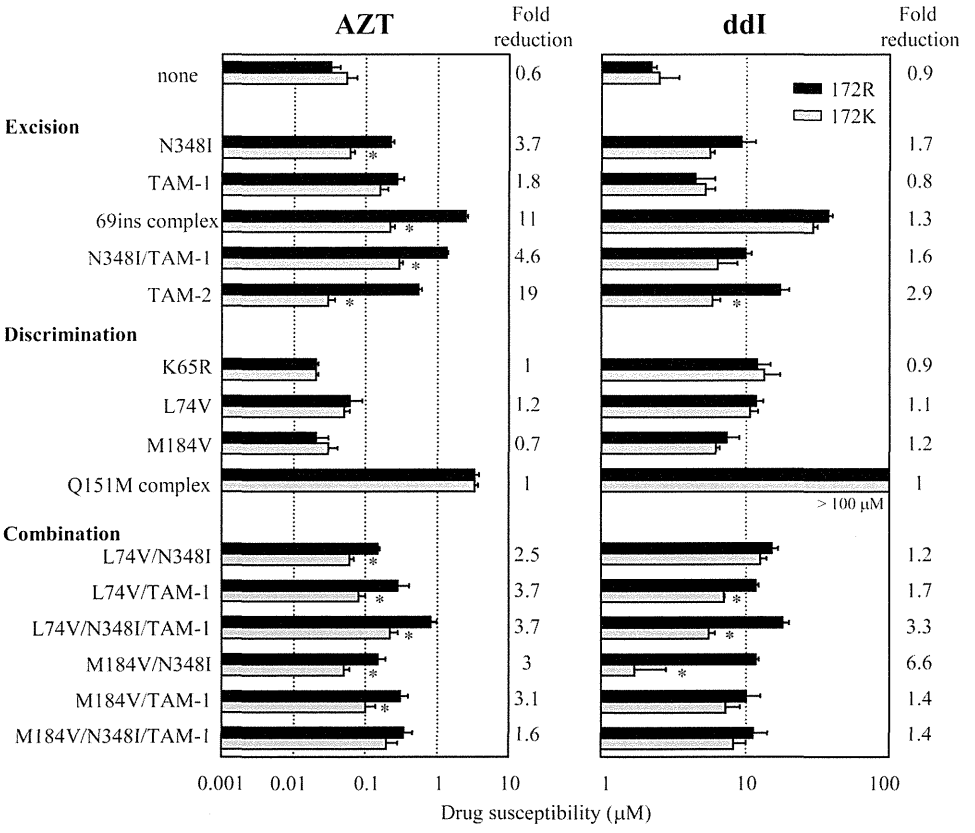

FIGURE 1. **Effect of the 172K polymorphism on HIV-1 susceptibility to AZT and ddI.** Antiviral activities of HIV-1 carrying NRTI resistance mutations with 172R (*black bars*) or 172K (*gray bars*) were determined by MAGIC-5 cell-based assay and shown as the concentration required for 50% inhibition of virus infection (EC_{50}). "TAM-1 and -2" have the "M41L and T215Y" and "D67N, K70R, T215F, and K219Q" mutations, respectively. 69ins complex carries 69 insertion and TAM-1. Q151Mc complex carries Q151M, A62V, V75I, F77L, and F116V. *Error bars* represent standard deviations from at least three independent experiments. *Asterisks* mark statistically significant differences ($p < 0.05$ by *t* test) in EC_{50} values comparing 172K with 172R in the background of NRTI-resistant mutations. Susceptibility of the Q151Mc complex with 172R or 172K to ddI was not assessed because the EC_{50} values were over the detection limit for this assay (>100 μM).

Structural Analysis—The program COOT was used to align crystal structure coordinates (typically using residues 107–112 and 151–215 of the p66 subunit) of the following complexes: RT_{172R} RT-EFV with RT_{172K} RT-EFV (PDB code numbers 1FK9 and 1IKW), $RT_{172R/K103N}$ RT-EFV with $RT_{172K/K103N}$ RT-EFV (PDB code numbers 1FKO and 1IKV), and RT_{172R} RT-NVP with RT_{172K} RT-U05 (a NVP analog) (PDB code numbers 1RTH and 3HVT). We also compared RT-DNA-dNTP ternary complexes (1RTD and 3JYT, as examples of RT_{172R} and RT_{172K} RTs). Figures were generated using PyMOL Molecular Graphics Program.

RESULTS

Effect of 172K on NRTI Resistance—To determine the effect of 172R or 172K on NRTI resistance, we generated RT_{172R} and RT_{172K} mutants carrying various NRTI-resistant mutations (Fig. 1 and supplemental Table 2) and compared the EC_{50} value of HIV-1_{172R} with that of HIV-1_{172K} in the background of NRTI-resistant mutations shown as a "fold reduction" in the Fig. 1. Although 172K alone had no effect on AZT or ddI susceptibility, 172K significantly reduced the AZT resistance of the following mutants that are associated with the excision mechanism: N348I, 69ins complex N348I/TAM-1 and TAM-2. Similarly, 172K appeared to suppress ddI resistance of a mutant that is associated with the excision mechanism TAM-2. In contrast, 172K had no statistically significant impact on AZT or ddI resistance of viruses with mutations that cause drug resistance by decreasing incorporation of NRTIs (K65R, L74V, M184V, and Q151Mc) (Fig. 1).

When we examined the effect of 172K on viruses that had combinations of mutations that cause NRTI resistance through the excision mechanism and through the decreased incorporation mechanism, we observed that 172K significantly suppressed resistance of L74V/TAM-1, L74V/N348I/TAM-1, and M184V/N348I, to AZT and to ddI (Fig. 1). These data suggested that 172K augments the suppressive effects of L74V and M184V on AZT and ddI resistance.

To further examine the effect of 172K on resistance to other Food and Drug Administration-approved NRTIs, we focused on the susceptibility of the 69ins complex to d4T, ABC, TDF, and 3TC (Table 1). Our data show that the 172K polymorphism significantly suppressed resistance of the 69ins complex to d4T (3-fold reduction; Table 1) and to AZT (11-fold reduction; Fig. 1). However, the resistance of 69ins complex to 3TC (54), ABC, and TDF was not significantly affected by 172K (less than 1.2-fold reduction in resistance). These results indicate that the suppressive effect of 172K can be NRTI-specific.

Effect of 172K on NNRTI Resistance—The antagonistic effects of 172K on the NNRTI resistance of RTs with mutations at K103N, V106M, V108I, Y181C, Y188L, and N348I are shown in Fig. 2 (and also supplemental Table 3). Fold reduction was

TABLE 1
Antiviral activities of NRTIs against HIV-1 encoding 69ins complex mutations in the background of 172K or 172R polymorphisms

Mutation(s)	EC_{50} (μM) (fold increase)[a]			
	d4T	ABC	TDF	3TC
172R	2.8 ± 0.9	2.7 ± 0.3	0.03 ± 0.01	1.5 ± 0.5
69ins complex/172R	16.7 ± 1.5 (6)	38.7 ± 3.1 (14)	0.16 ± 0.01 (5)	16.0 ± 1.0 (11)
69ins complex/172K	5.5 ± 1.3 (2)[b]	35.7 ± 2.5 (13)	0.13 ± 0.03 (4)	14.0 ± 1.0 (9)

[a] Values are means from at least three independent experiments, and the relative increase in the EC_{50} value for recombinant viruses compared with 172R is shown in parentheses.
[b] EC_{50} of 69ins complex with 172K is significantly different from that with 172R ($p < 0.0006$ by t test).

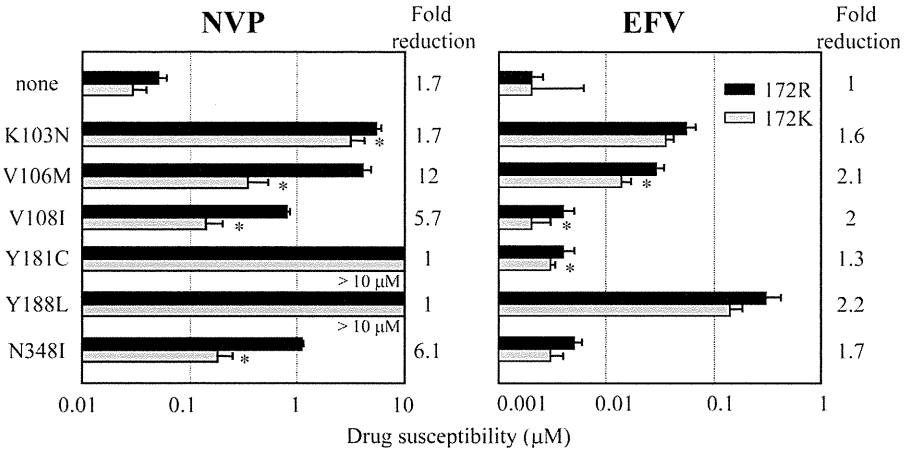

FIGURE 2. **Effect of the 172 polymorphism on HIV-1 susceptibility to NVP and EFV.** Antiviral activities of HIV-1 carrying NNRTI resistance mutations with 172R (*black bars*) or 172K (*gray bars*) were determined by MAGIC-5 cell-based assay and shown as the concentration required for 50% inhibition of virus infection (EC_{50}). *Error bars* represent standard deviations from at least three independent experiments. *Asterisks* mark statistically significant differences ($p < 0.05$ by t test) in EC_{50} values comparing 172K with 172R in the background of NNRTI-resistant mutations. Susceptibilities of Y181C or Y188L with 172R or 172K to NVP were not assessed because their EC_{50} values were over the detection limit for this assay (>10 μM).

TABLE 2
Primer extension assay of RT inhibition by AZT in the presence or absence of ATP

HIV-1 RT	IC_{50} of AZT-TP (nM)[a] (-fold increase)[b]		Excision enhancement by ATP[c]
	Without ATP	With ATP	
172R	286 ± 30 (1)	359 ± 18 (1)	1.3
172K	148 ± 5 (0.52)	183 ± 13 (0.52)	1.2
172R/TAM-2[d]	250 ± 20 (0.87)	995 ± 126 (2.78)	4.0
172K/TAM-2[d]	290 ± 19 (1.01)	517 ± 36 (1.44)	1.8

[a] The data are means ± S.D. from at least three independent experiments.
[b] Fold increase was compared with each WT 172R (without/with ATP).
[c] Excision enhancement by ATP is calculated as (IC_{50} with ATP)/(IC_{50} without ATP).
[d] TAM-2 carries D67N, K70R, T215F, and T219Q.

calculated as "EC_{50} of 172R/EC_{50} of 172K." 172K significantly suppressed NVP resistance conferred by K103N, V106M, V108I, and N348I. The impact of 172K on NVP resistance in the context of Y181C or Y188L could not be assessed, because both exhibited very high resistance (>10 μM) under these conditions. 172K also reduced EFV resistance of V106M, V108I, and Y181C. Hence, the impact of 172K on EFV resistance was considerably lower than that on NVP resistance. Collectively, our data demonstrate that RT resistance to NNRTIs (especially to NVP) can also be affected by 172K. A similar effect has been observed in assays using purified RTs containing either 172R or 172K. A lysine at position 172 conferred a higher susceptibility to NVP, while displaying only marginal differences for EFV, etravirine, and rilpivirine when compared with RT containing an arginine at that position (data not shown).

Effect of 172K on AZT Resistance of HIV-1 RT—TAMs cause AZT resistance by enhancing the ability of RT to remove the terminal AZT-monophosphate (AZT-MP) from the 3′-primer terminus using a pyrophosphate donor such as ATP. To determine whether 172K suppresses AZT resistance through a reduction in the efficiency of ATP-mediated excision, we purified RT_{172R} and RT_{172K} with TAM-2. We measured the susceptibility of RTs to inhibition by AZT in the presence or absence of ATP in a primer extension assay that uses long T/P (T_{100}/5′-Cy3-P_{18long}) (Table 2 and also supplemental Fig. 1). Any changes in AZT susceptibility *only* in the presence of ATP would suggest that the effect is excision-dependent. $RT_{172R/TAM-2}$ showed ~4-fold higher IC_{50} in the presence of ATP (995 *versus* 250 nM), although $RT_{172K/TAM-2}$ exhibited only a 1.8-fold excision enhancement by ATP (517 *versus* 290 nM). Hence, the ATP-based (or excision-based) increase in AZT resistance in TAM-2 was at least twice as much in the presence of 172R than 172K (4-fold *versus* 1.8-fold excision enhancement). However, in the absence of TAMs the effect of ATP was comparable for RT_{172R} and RT_{172K} (1.3-fold *versus* 1.2-fold excision enhancement) and smaller than in the case of the TAM enzymes. To further confirm these results, we also performed ATP-rescue assay using $RT_{172R/TAM-2}$

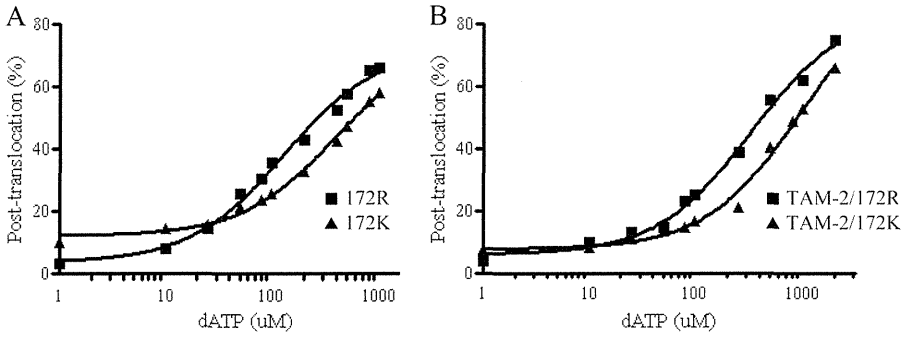

C

	172R	172K	TAM-2/172R	TAM-2/172K
Concentration of dATP needed to translocate 50% of RT / [μM]	128	388	327	940

FIGURE 3. **Effect of the 172 polymorphism on the translocation state of various HIV-1 RTs.** The effect of added dNTP on the translocation site of HIV-1 RT is compared for 172R (■) and 172K (▲) (*A*), as well as for TAM-2/172R (■) and TAM-2/172K (▲) (*B*). Complexes of RT with a double-stranded DNA terminated by a dideoxynucleotide were mixed with different concentrations of dATP eventually forming dead end complexes that position the nucleic acid in a post-translocation site. The dead end complexes were treated with hydroxyl radicals prepared in the presence of Fe^{2+}, and the nucleic acids were cleaved at position −18 or −17, depending on whether they were bound in a pre- or a post-translocation site. We quantified the bands in post- and pre-translocation sites and plotted the percent translocation. The concentrations of dATP required to translocate by 50% are shown in *C*.

and $RT_{172K/TAM-2}$. The rescue assays involve unblocking of AZT-terminated primers through ATP-based excision and DNA synthesis. $RT_{172K/TAM-2}$ also decreased ATP-excision reactions (data not shown). Hence, the suppressive effect of 172K in AZT resistance is ATP excision-dependent.

Effect of 172K on the Translocation Site of HIV-1 RT Measured by Fe^{2+} Footprinting—A single cycle of DNA polymerization involves dNTP binding, incorporation, and translocation of the elongated DNA primer from the dNTP-binding site (pre-translocation site, N-site) to the priming site (post-translocation site, P-site). For efficient ATP-based excision, the AZT-MP-terminated primer needs to be positioned at the pre-translocation site (14, 47). To determine whether 172K influences the positioning of AZT-MP-terminated primers, we performed a site-specific Fe^{2+} footprinting assay (Fig. 3). We mixed various RTs with AZT-terminated DNA and different concentrations of the incoming dATP substrate to form dead end complexes that position DNA in a post-translocation site. Treatment with hydroxyl radicals prepared in the presence of Fe^{2+} allowed cleavage at positions that correspond to pre- or post-translocation sites, and we monitored translocation as a function of dATP required to translocate 50% of RT. In this assay, lower numbers indicate more efficient translocation. Our data indicated that $RT_{172R/TAM-2}$ (or $RT_{172K/TAM-2}$) required higher dATP concentrations than RT_{172R} (or RT_{172K}) to translocate by 50% (327 *versus* 128 μM or 940 *versus* 388 μM). These data are consistent with previous reports that AZT-resistant RTs with excision mutations primarily bind in a pre-translocation site (47) and is thus more accessible for ATP-based excision. Interestingly, although $RT_{172K/TAM-2}$ has suppressed AZT resistance compared with $RT_{172R/TAM-2}$, it still bound the AZT-MP-terminated primer more efficiently in an excision-competent pre-translocation site (940/327 = 2.9-fold). Taken together, our data suggest that the decreased excision by 172K is *not* due to repositioning of the AZT-MP-terminated primer at the nonexcisable post-translocation site.

DNA Binding by HIV-1 RT Measured by Surface Plasmon Resonance—We hypothesized that the decreased excision-based resistance of 172K is due to a more efficient dissociation of the nucleic acid substrate, such that it decreases the opportunities to unblock chain terminated primers, thus resulting in suppression of AZT resistance. Hence, we used SPR to measure DNA binding and compare the DNA binding affinities of RT_{172K} and RT_{172R}. We chose SPR because measurements of the dissociation constant, $K_{D.\,DNA}$, using gel-mobility shift assays, do not offer insights regarding the kinetics of binding (k_{on}) and release (k_{off}) of nucleic acid from the enzyme. We attached biotinylated DNA on a streptavidin sensor chip and flowed various concentrations of either enzyme over the chip to measure the association (k_{on}) and dissociation (k_{off}) rates of the enzymes in real time (Fig. 4). The k_{off} value for RT_{172K} was markedly increased (31-fold) with a slightly changed k_{on} value (2.9-fold) compared with those for RT_{172R}. The $K_{D.\,DNA}$ ($=k_{off}/k_{on}$) value for RT_{172K} was 11-fold higher than that for RT_{172R} (1.8 and 0.16 nM, respectively). Our results demonstrate that RT_{172K} had lower DNA binding affinity than RT_{172R} due to a significant difference in the dissociation rate of RT from the DNA.

Processivity of HIV-1 RT—Considering that low DNA binding affinity by 172K may contribute to decreased processivity, we carried out processivity assays using RT_{172K} or RT_{172R} in the absence or presence of the NRTI resistance background. Assays were carried out using a long DNA template in the presence of heparin as a competitive trap (Fig. 5). Full-length product formation was less observed in RT_{172K} compared with RT_{172R}, indicating that 172K attenuates processivity. When introduced into RT_{TAM-2}, 172K lowered processivity even more. In contrast, Q151Mc may enhance RT processivity, as Q151Mc was more processive than WT, especially in the presence of RT_{172K}. These data suggest that 172K could decrease RT processivity in the background of only excision and not discrimination resistance mutations.

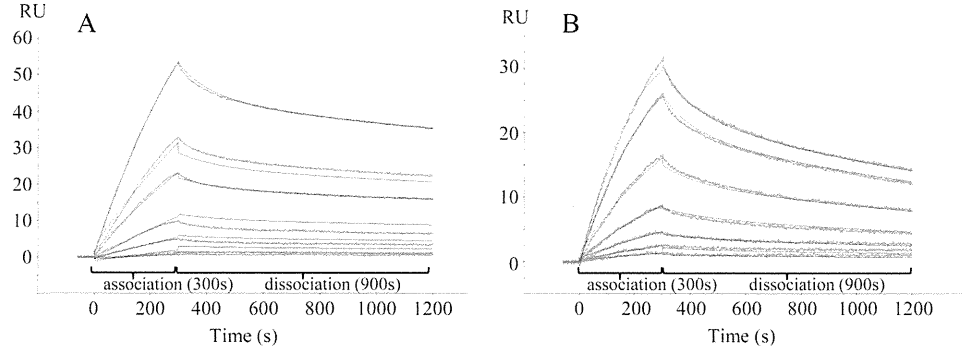

C

HIV-1 RT	K_d (nM)	k_{on} ($s^{-1}M^{-1}$)	k_{off} (s^{-1})
172R	0.16	8.3×10^4	1.4×10^{-5}
172K	1.8	2.4×10^5	4.3×10^{-4}

FIGURE 4. **Assessment of $K_{D,\ DNA}$, k_{on}, and k_{off} using SPR.** SPR was used to measure the DNA binding affinity of RTs with an arginine or a lysine at codon 172 (172R in *A* and 172K in *B*). Increasing concentrations (0.5, 1, 2, 4, 7.5, 10, 15, and 20 nM) of each RT were flowed over a streptavidin chip with biotinylated double-stranded DNA (5′-biotin-T_{d37}/P_{d25}) immobilized on its surface as described under "Experimental Procedures." The experimental trace (*red*) shown is the result of a subtraction of the data obtained from the channel containing the immobilized DNA minus the signal obtained from a control/background channel. DNA binding constants for RT_{172R} or RT_{172K} are shown in *C*.

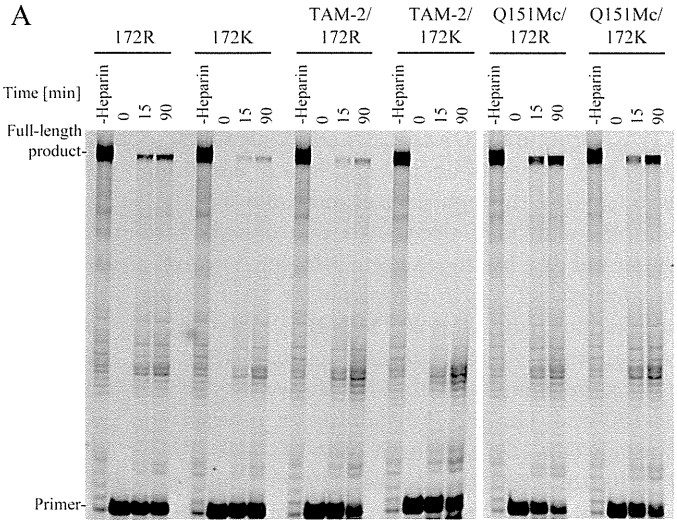

B

HIV-1 RT	Full-length DNA synthesis at 90 min (%)	
	172R	172K
none	8.4	3.2
TAM-2	3.5	0.2
Q151Mc	21.9	18.4

FIGURE 5. **Effect of changes at codon 172 on the processivity of HIV-1 RT.** *A*, processive DNA synthesis was measured at 0, 15, and 90 min after initiation of the reaction in the presence of heparin trap for each RT enzyme (WT, TAM-2, and Q151Mc) with 172R or 172K. Conditions were selected so that in the absence of heparin trap (*1st lane* of every set, labeled as *−Heparin*), the sum of processive and distributive DNA synthesis was the same (comparable full-length product in *−Heparin* lanes). All experiments were repeated three times and a representative gel is shown here. *B*, amount of full-length extended and un-extended products at 90 min after initiation of the reaction were quantified by densitometry using MultiGauge. Percentages of full-length DNA synthesis are shown in *B*.

TABLE 3
dATP incorporation under steady state conditions

HIV-1 RT	K_m	k_{cat}	k_{cat}/K_m
	nM	min^{-1}	$min^{-1} \cdot nM^{-1}$
172R	132	4.2	0.03
172K	143	7.2	0.05

TABLE 4
NVP susceptibility assay at the enzyme and virus level

Mutation	IC_{50} of NVP,[a] Enzyme (RT)[c]	EC_{50} of NVP,[a] HIV virus[b]
	nM	nM
172R	965 ± 55 (1)[b]	50 ± 10 (1)[b]
172K	174 ± 46 (0.2)[b]	30 ± 10 (0.6)[b]
172R/V106M	54795 ± 5565 (57)[b]	4100 ± 760 (83)[b]
172K/V106M	6181 ± 1096 (6)[b]	350 ± 190(7)[b]

[a] The data are means ± S.D. from at least three independent experiments.
[b] Fold increase was compared with WT 172R.
[c] These data were obtained from primer extension assay in the presence of NVP.
[d] These data were obtained from cell-based assay using MAGIC-5.

Steady State Kinetics of Nucleotide Incorporation—Initial polymerase activity comparisons of RT_{172R} and RT_{172K} showed that 172K slowed the polymerase activity of RT. This observation led us to investigate the steady state nucleotide incorporation properties of RT_{172R} and RT_{172K} using single nucleotide incorporation assays (Table 3). The estimated values for k_{cat} and $K_{m.dNTP}$ show that RT_{172K} and RT_{172R} had comparable efficacies ($k_{cat}/K_{m.dNTP}$ of 0.05 *versus* 0.03 min^{-1} nM^{-1}) under steady state conditions. These data suggested that 172K decreased RT processivity without affecting catalytic efficiency for nucleotide incorporation.

Susceptibility of HIV-1 RT to NVP—To examine the suppressive effect of 172K on NNRTI resistance at the HIV-1 RT enzyme level, we purified HIV-1 RT with V106M in the background of Arg or Lys at RT codon 172 and performed primer extension assays in the presence of NVP (Table 4). When introduced into RT_{V106M}, 172R results in an enzyme ($RT_{172R/V106M}$) with 57-fold resistance to NVP. In contrast, $RT_{172K/V106M}$ showed decreased resistance to NVP (6-fold). Hence, the extent of the suppressive effect of 172K on NVP resistance at the enzyme level was comparable with the effect observed at the virus level.

Crystal Structure of HIV-1 RT with Mutation at Codon 172—The structure of RT with the K172A mutation was determined at 2.15 Å resolution (supplemental Table 1). This is one of the

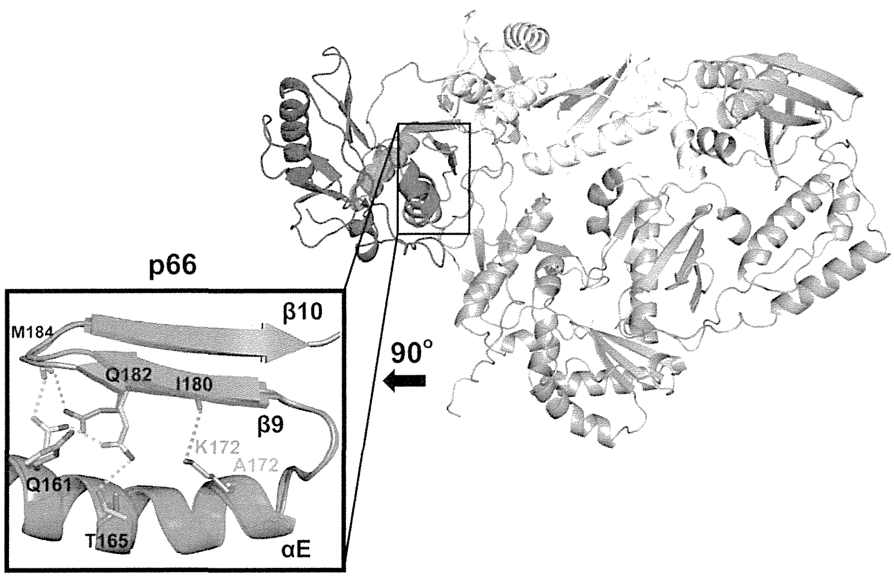

FIGURE 6. **Structural comparison of unliganded HIV-1 RT structures with Lys or Ala at codon 172.** HIV-1 RT with 172 mutated to alanine (PDB code 4DG1) is shown superposed to HIV-1 RT containing a 172K (PDB code 1DLO). Noticeable changes are observed in the hydrogen bond network between residues from α-helix E (161, 165, and 172) and from β9-strand (180, 182, and 184). The p66 palm subdomains of RT containing 172K or 172A are shown in *light blue* and *red*, respectively.

highest resolution structures of HIV-1 RT. In addition to this mutation, RT had also the K173A mutation to improve the crystallographic properties of the enzyme (48). However, we confirmed K173A did not affect susceptibility of RT to NVP and AZT, and it also did not alter the effect of the 172R or 172K change to susceptibility to RTIs at the virus or at the enzyme level (data not shown). The overall conformation of the mutant RT is similar to that of WT unliganded RT in which the p66 thumb subdomain is folded down into the DNA binding cleft (55). However, there are notable changes proximal to mutated residue 172 of the α-helix E, which affect interactions with residues of the β9-strand that leads to the YMDD loop of the polymerase active site. The Lys-172–Ile-180 interaction is lost in the 172A structure. This change is accompanied by a repositioning of the amide side chain of Gln-182, which in the 172K structure stabilizes the Met-184 main chain amide of the YMDD loop, whereas in the 172A structure it makes hydrogen bonds with the Thr-165 hydroxyl group and the Gln-161 side chain amide. Hence, the changes in the interactions between 172 and 180 propagate toward the polymerase active site (Fig. 6).

Effect of 172K on the Structure of HIV-1 RT—To further examine how 172K can simultaneously decrease to both NRTI and NNRTI resistances, we performed structural comparisons by aligning the crystal structures of RT_{172R} and RT_{172K} RTs in complex with NNRTIs. Interestingly, the structural changes observed among RT complexes that have different amino acids at position 172 follow the same pattern, albeit with small variations, as we observed in the comparisons among the unliganded structures (see above). In all cases, 172K and 172R of the α-helix E interact differently with residue 180 of the β9-strand, and this change affects in turn interactions between other residues of these structural elements as follows: 161 and 165 of the α-helix E, with 182 and 184 of the β9-strand (Fig. 7). Specifically, the RT_{172R} structure in complex with NVP shows that 172R and Gln-161 in α-helix E interact with Ile-180 and Gln-182 and indirectly with Met-184 in the β9-strand (Fig. 7*A*). The RT_{172R} structure in complex with EFV also shows that the 172R side chain contacts Ile-180 and has an additional interaction with Gln-182 through a water molecule (Fig. 7*B*). The RT_{172R} complex with EFV also shows that α-helix E helps stabilize β9-strand by a hydrogen bond between Thr-165 and Gln-182. In contrast, RT_{172K} in complex with NVP analog U05 has no interactions with Ile-180, Met-184, and Gln-161, following repositioning of surrounding residues (Fig. 7*A*). Similarly, RT_{172K} in complex with EFV shows loss of interactions of Ile-180 and Thr-165, but additional interactions are gained through Gln-161 with both Met-184 and Gln-182 (Fig. 7*B*). This loss of interaction between 172K and Ile-180 and Gln-182 is also observed in the presence of nucleic acid substrate (Fig. 7*C*). Furthermore, in the reported crystal structure of $RT_{172R/K103N}$, the aromatic side chain of Tyr-181 seems to flip almost 90° in the opposite direction and is likely to affect NNRTI susceptibility (Fig. 7*D*). Taken together, this information suggests that the residues in α-helix E may be involved in stabilizing the β9-strand, which is a part of the polymerase active site where NRTIs bind and of the NNRTI binding pocket. Changes in the interactions between the residues of α-helix E and β9-strand may affect the positioning of the YMDD loop, thus affecting not only NRTI and NNRTI binding but also substrate or DNA binding. This is consistent with previous reports on reduction of RT processivity due to changes in the YMDD loop (56, 57).

DISCUSSION

Our virological and biochemical data demonstrate that 172K suppresses resistance to both NRTIs and NNRTIs. Moreover, we established that the suppression of NRTI resistance by 172K involves a decrease in ATP-mediated excision. Previous studies have demonstrated that some NRTI and NNRTI resistance mutations can also affect excision-based NRTI resistance.

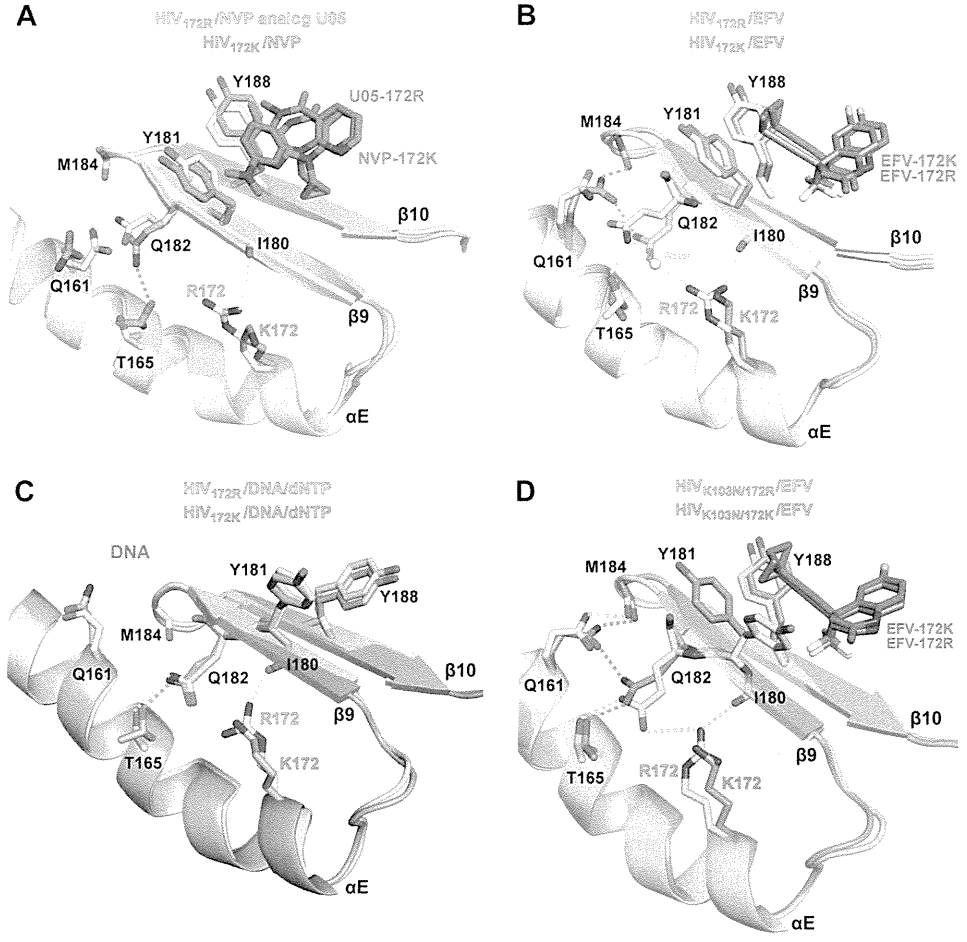

FIGURE 7. **Structural comparison of HIV-1 RT complexes with Lys or Arg at codon 172.** *A*, comparison of RT_{172R} (*cyan* side chains and *ribbons*) bound to NVP analog U05 (*blue sticks*) *versus* RT_{172K} (*pink side chains* and *ribbons*) bound to NVP (*pink sticks*). The change of 172R (*cyan*) to 172K (*pink*) affects the interactions between side chains of β-9–10 sheet and α-helix E. *B*, comparison of RT_{172R} (*cyan* side chains and *ribbons*) bound to EFV (*blue sticks*) *versus* RT_{172K} (*pink* side chains and *ribbons*) bound to EFV (*red sticks*). Similarly to *A*, the 172K → 172R change affects the intermolecular interactions between side chains of β-9–10 sheet and α-helix E. *C*, comparison of RT_{172R} (*cyan* side chains and *ribbons*) and RT_{172K} (*pink* side chains and *ribbons*) complexes with DNA and dNTP (not shown). *D*, comparison of $RT_{K103N/172R}$ (*cyan* side chains and *ribbons*) bound to EFV (*blue sticks*), and $RT_{K103N/172K}$ (*pink* side chains and *ribbons*) bound to EFV (*red sticks*). In addition to changes in the interactions between side chains of β-9–10 sheet and α-helix E also observed in *A* and *B*, the side chain of Tyr-181 "flips" in the 172K *versus* the 172R structure.

Hence, NRTI resistance mutations K65R, K70E, L74V, and M184V and NNRTI resistance mutations L100I and Y181C block ATP-mediated excision and suppress AZT resistance (32–35, 37, 38). In contrast, other NRTI resistance mutations (V118I and T215Y) impart NNRTI hyper-susceptibility to HIV-1 (58). To our knowledge, 172K is the first polymorphism that suppresses resistance to two independent types of inhibitors, NRTIs and NNRTIs.

Pathak and co-workers (24–27) proposed that connection subdomain mutations enhance NRTI and NNRTI resistance by reducing RNase H activity, thereby providing additional time for RT to bind in an NRTI excision-competent mode or allow NNRTIs to dissociate from RT (RNase H-dependent resistance mechanism). It is likely that connection subdomain mutations can also cause RNase H-independent AZT resistance. For example, mutation G333D does not reduce RNase H function, but it increases ATP-mediated excision, likely the result of long range interactions (27, 59). In addition, N348I confers NRTI and NNRTI resistance and increases ATP-mediated excision of AZT by both RNase H-dependent and independent mechanisms (60). The antagonistic effects of Y181C or M184V on phenotypic AZT resistance cannot be counteracted by N348I (19, 61). Interestingly, 172K reduces the resistance (to NRTIs or NNRTIs) that N348I imparts to HIV when added to WT, L74V, L74V/TAM-1, M184V, or M184V/TAM-1 backgrounds (Fig. 1). We showed that 172K can either slightly increase (RT_{172K} *versus* RT_{172R}) or decrease ($RT_{172K/TAM-2}$ *versus* $RT_{172R/TAM-2}$) the RNase H activity (supplemental Fig. 2). Hence, 172K does not have a consistent effect on RNase H function and is thus unlikely to reduce NRTI or NNRTI resistance by restoring the RNase H defect introduced by N348I.

How then is 172K reducing NRTI resistance? There are several possible mechanisms by which a residue could enhance susceptibility to NRTIs. First, it could improve NRTI incorporation into DNA. However, this is not the case with 172K because the IC_{50} values for AZT inhibition of $RT_{172R/TAM-2}$ or $RT_{172K/TAM-2}$ are not significantly different under conditions where only incorporation and not excision are examined (in the absence of ATP) (Table 2 and also supplemental Fig. 1). Second, a residue could increase sensitivity to NRTIs by decreasing excision. This could be accomplished by several ways including the following: (*a*) by promoting translocation of the NRTI-ter-

minated primer to the post-translocation site (47), which is not accessible to ATP, thus preventing NRTI excision (47). This is also not the case with 172K, as RT_{172K} favors the pre-translocated mode of binding (Fig. 3), which allows unblocking of chain-terminated primers; (*b*) by decreasing the excision efficiency through impaired use of the excision substrate ATP. However, our data (not shown) do not support this possibility, as we do not find any significant difference in ATP binding between $RT_{172R/TAM-2}$ and $RT_{172K/TAM-2}$ or RT_{172R} and RT_{172K} (the apparent K_m for ATP in a rescue-type assay for all enzymes is ~3 mM); (*c*) by increasing the dissociation of chain-terminated T/P, thereby limiting unblocking. Our data are consistent with this apparently novel mechanism of suppression of NRTI resistance. Specifically, SPR measurements indicate that RT_{172K} had decreased affinity for nucleic acid due to an increased dissociation rate (Fig. 4) (k_{off} was ~31-fold higher in the case of RT_{172K}). Hence, our data suggest that RT_{172K} has decreased AZT resistance primarily because the AZT-terminated template/primer falls off of the enzyme and cannot be unblocked. This is also consistent with the observed decrease in processivity of RT_{172K} and $RT_{172K/TAM-2}$ (Fig. 5). Interestingly, the processivity of $RT_{172K/Q151Mc}$ was not reduced (Fig. 5). Hence, it is possible that the relatively higher prevalence of $RT_{172K/Q151Mc}$ (9.9%, supplemental Table 4) compared with $RT_{172K/TAM-2}$ is likely due to the higher processivity and presumably higher fitness of $RT_{172K/Q151Mc}$.

The structural basis of decreased NNRTI resistance and AZT excision by RT_{172K} is likely related to how changes at 172 affect the positioning and mobility of the active site YMDD loop during the course of polymerization. The structural analysis of the crystal structures solved here and previously (Figs. 6 and 7) predict some changes in the interactions of the β9-strand with the α-helix E. The changes are propagated toward the polymerase active site and may affect the relative motions of the YMDD loop during the course of polymerization. Our previously published work has established that the mobility of YMDD is important for NRTI excision, processivity (57), and NNRTI susceptibility (56). Hence, it is possible that 172K affects NRTI and NNRTI resistance by changing the local environment of YMDD.

The R172K change emerges during serial passages of HIV-1 in MT-2 cells in increasing concentrations of Reverset (RVT, D-2′,3′-didehydro-2′,3′-dideoxy-5-fluorocytidine), a nucleoside analog with potent activity against HBV and AZT-resistant HIV-1, especially in the presence of TAMs (62, 63). Phenotypic analysis revealed that K70N/V90I/R172K had a 3.9-fold increase in RVT resistance (64). Our findings indicate that appearance of 172K during RVT therapy may also affect resistance to other drugs and should be taken into consideration in designing RVT-based therapeutic strategies.

In conclusion, we have identified the first RT polymorphism that suppresses resistance to both NRTIs and NNRTIs. The effect of polymorphisms in suppressing NRTI and NNRTI resistance provides new information into the interactions between the polymerase active site and the NNRTI-binding site of RT. These findings provide valuable insights for the design of antiviral regimens and new RT inhibitors.

REFERENCES

1. Mitsuya, H., Yarchoan, R., and Broder, S. (1990) Molecular targets for AIDS therapy. *Science* **249,** 1533–1544
2. Furman, P. A., Fyfe, J. A., St Clair, M. H., Weinhold, K., Rideout, J. L., Freeman, G. A., Lehrman, S. N., Bolognesi, D. P., Broder, S., Mitsuya, H., *et al.* (1986) Phosphorylation of 3′-azido-3′-deoxythymidine and selective interaction of the 5′-triphosphate with human immunodeficiency virus reverse transcriptase. *Proc. Natl. Acad. Sci. U.S.A.* **83,** 8333–8337
3. Singh, K., Marchand, B., Kirby, K. A., Michailidis, E., and Sarafianos, S. G. (2010) Structural aspects of drug resistance and inhibition of HIV-1 reverse transcriptase. *Viruses* **2,** 606–638
4. Sarafianos, S. G., Marchand, B., Das, K., Himmel, D. M., Parniak, M. A., Hughes, S. H., and Arnold, E. (2009) Structure and function of HIV-1 reverse transcriptase. Molecular mechanisms of polymerization and inhibition. *J. Mol. Biol.* **385,** 693–713
5. de Clercq, E. (1996) Non-nucleoside reverse transcriptase inhibitors (NNRTIs) for the treatment of human immunodeficiency virus type 1 (HIV-1) infections. Strategies to overcome drug resistance development. *Med. Res. Rev.* **16,** 125–157
6. Spence, R. A., Kati, W. M., Anderson, K. S., and Johnson, K. A. (1995) Mechanism of inhibition of HIV-1 reverse transcriptase by non-nucleoside inhibitors. *Science* **267,** 988–993
7. Deval, J., Selmi, B., Boretto, J., Egloff, M. P., Guerreiro, C., Sarfati, S., and Canard, B. (2002) The molecular mechanism of multidrug resistance by the Q151M human immunodeficiency virus type 1 reverse transcriptase and its suppression using α-boranophosphate nucleotide analogs. *J. Biol. Chem.* **277,** 42097–42104
8. Deval, J., Navarro, J. M., Selmi, B., Courcambeck, J., Boretto, J., Halfon, P., Garrido-Urbani, S., Sire, J., and Canard, B. (2004) A loss of viral replicative capacity correlates with altered DNA polymerization kinetics by the human immunodeficiency virus reverse transcriptase bearing the K65R and L74V dideoxynucleoside resistance substitutions. *J. Biol. Chem.* **279,** 25489–25496
9. Huang, H., Chopra, R., Verdine, G. L., and Harrison, S. C. (1998) Structure of a covalently trapped catalytic complex of HIV-1 reverse transcriptase. Implications for drug resistance. *Science* **282,** 1669–1675
10. Sarafianos, S. G., Pandey, V. N., Kaushik, N., and Modak, M. J. (1995) Glutamine 151 participates in the substrate dNTP binding function of HIV-1 reverse transcriptase. *Biochemistry* **34,** 7207–7216
11. Sarafianos, S. G., Das, K., Clark, A. D., Jr., Ding, J., Boyer, P. L., Hughes, S. H., and Arnold, E. (1999) Lamivudine (3TC) resistance in HIV-1 reverse transcriptase involves steric hindrance with β-branched amino acids. *Proc. Natl. Acad. Sci. U.S.A.* **96,** 10027–10032
12. Boyer, P. L., Sarafianos, S. G., Arnold, E., and Hughes, S. H. (2001) Selective excision of AZTMP by drug-resistant human immunodeficiency virus reverse transcriptase. *J. Virol.* **75,** 4832–4842
13. Meyer, P. R., Matsuura, S. E., So, A. G., and Scott, W. A. (1998) Unblocking of chain-terminated primer by HIV-1 reverse transcriptase through a nucleotide-dependent mechanism. *Proc. Natl. Acad. Sci. U.S.A.* **95,** 13471–13476
14. Tu, X., Das, K., Han, Q., Bauman, J. D., Clark, A. D., Jr., Hou, X., Frenkel, Y. V., Gaffney, B. L., Jones, R. A., Boyer, P. L., Hughes, S. H., Sarafianos, S. G., and Arnold, E. (2010) Structural basis of HIV-1 resistance to AZT by excision. *Nat. Struct. Mol. Biol.* **17,** 1202–1209
15. Arion, D., Kaushik, N., McCormick, S., Borkow, G., and Parniak, M. A. (1998) Phenotypic mechanism of HIV-1 resistance to 3′-azido-3′-deoxythymidine (AZT). Increased polymerization processivity and enhanced sensitivity to pyrophosphate of the mutant viral reverse transcriptase. *Biochemistry* **37,** 15908–15917
16. Lin, P. F., Samanta, H., Rose, R. E., Patick, A. K., Trimble, J., Bechtold, C. M., Revie, D. R., Khan, N. C., Federici, M. E., Li, H., *et al.* (1994) Genotypic and phenotypic analysis of human immunodeficiency virus type 1 isolates from patients on prolonged stavudine therapy. *J. Infect. Dis.* **170,** 1157–1164
17. Larder, B. A., and Kemp, S. D. (1989) Multiple mutations in HIV-1 reverse transcriptase confer high level resistance to zidovudine (AZT). *Science* **246,** 1155–1158
18. Nikolenko, G. N., Delviks-Frankenberry, K. A., Palmer, S., Maldarelli, F.,